POLITECNICO DI TORINO

Department of mechanical and aerospace engineering

Master of science in Mechanical engineering

Final project thesis

Synthetic cooling jet: design and efficiency analysis

Supervisor
Prof. Pietro Asinari

Hosting institution

Singapore Institute of Manufacturing Technology - SIMTech

Hosting institution supervisor
Dr. Jonathan Hey

Candidate
Pierluigi Nichilo

December 2018

ACKNOWLEDGEMENTS

A special acknowledgement is addressed to Dr. Jonathan Hey for supervising my experimental work at the Singapore Institute of Manufacturing Technology (SIMTech). He constantly coordinated my activities, providing me the fundamental guidelines at the base of the my thesis work and its achievements. I am grateful to him as a person for supporting me in settling in Singapore.

I would like to thank Prof. Asinari, who gave me the great opportunity to develop my Master thesis at the above mentioned institute. His great experience was fundamental in order to select and achieve the targets of the whole activity; furthermore, he demonstrated to be a great and careful man by always ensuring I was in the material and psychological condition to work at my best.

I will never acknowledge enough my family. My father and mother always provided me the necessary support to afford all the activities I decided to perform during my Master of Science. That is because they relied on my choices, believing I would have done the best for my future. I also send a big kiss to my sister Gabriella, who supported me in my everyday activities taking care of me whenever I was at home.

I would like to address hugs and kisses to all the friends I met in Singapore, since I spent amazing and unforgettable times with them, guaranteeing me the ability to work at my best.

Finally, a great contributor behind the curtains, Fanny. Her presence has been unbelievably encouraging this specific thesis work. She has been sitting close to me most of the hours dedicated to the writing of this document, falling asleep on my legs at 4 or 5 am, while I was still writing. She give me company, courage and strength in difficult moments. I am grateful to her for the energy she fed me.

PREFACE

In the last decades the industrial world was completely revolutionized by a massive usage of electronic devices.

Firstly, the usage of domestic and portable devices with microchips increased exponentially in consumers' good markets. At the same time, the digital transformation and the need for automated systems in the industrial world make so that electronics systems play a crucial role in any application of the domain. Such massive usage introduced the needs for downsizing and performance increasing, determining the introduction of high-density power electronics circuits in the markets.

Consequently, advanced electronic systems such as tablets, laptops, slim TV and industrial embedded systems carry challenging heat fluxes. Being the temperature level the main variable determining the life and the reliability of any electronic device, it can be justified the high amount of investments in research and development on the topic made by many manufacturers in the electronics field, as General Electric between the main ones.

The high heat fluxes characterizing compact thermal devices are so that the main features needed for a cooling device are: low cost, compactness, reliability and constructive easiness. Liquid cooling has shown great limits regarding those constraints, while synthetic jets on the contrary proved to be highly promising.

In the field of electronics, such a denomination generally refers to meso-scale devices generating the periodic suction and ejection of the fluid in which they are embedded, better called the medium. An intense small-scale turbulent jet is synthesized through it and in most of the cases the medium is a gas. Those devices do not transfer the mass of the fluid outside their control volume, but rather determine changes in momentum within it. For this specific reason they are likely to be referred as systems operating according the "zero-net-mass-flux principle".

The hereby presented work will focus on a synthetic cooling jet carrying a pulsating flow of ambient air over an heated copper plate, with the latter simulating the behavior of an electronic circuit. Different design configurations will be discussed, and so will be done for the characterization of the synthetic jet behavior, at different operating conditions.

A non-dimensional analysis will allow to extract precious information within the fluid dynamics, the acoustics and the thermodynamics domains, so that the study

here reported could be easily extended to other devices under appropriate similarities conditions.

INDEX

1|*SYNTHETIC JETS*

The main purpose of this chapter is to present synthetic jets main features and their most relevant applications. Furthermore, hereby will be explained the reasonable for carrying on this research work, as investing in synthetic jets looks promising for the industry, not only the electronics one due to recent importance in reducing wasted energy. Efficiency is an important answer to guarantee sustainable development in the actual industrial scenario, with markets continuously increasing in size and demand, but pressed by the new and upcoming worldwide regulations on environmental matters.

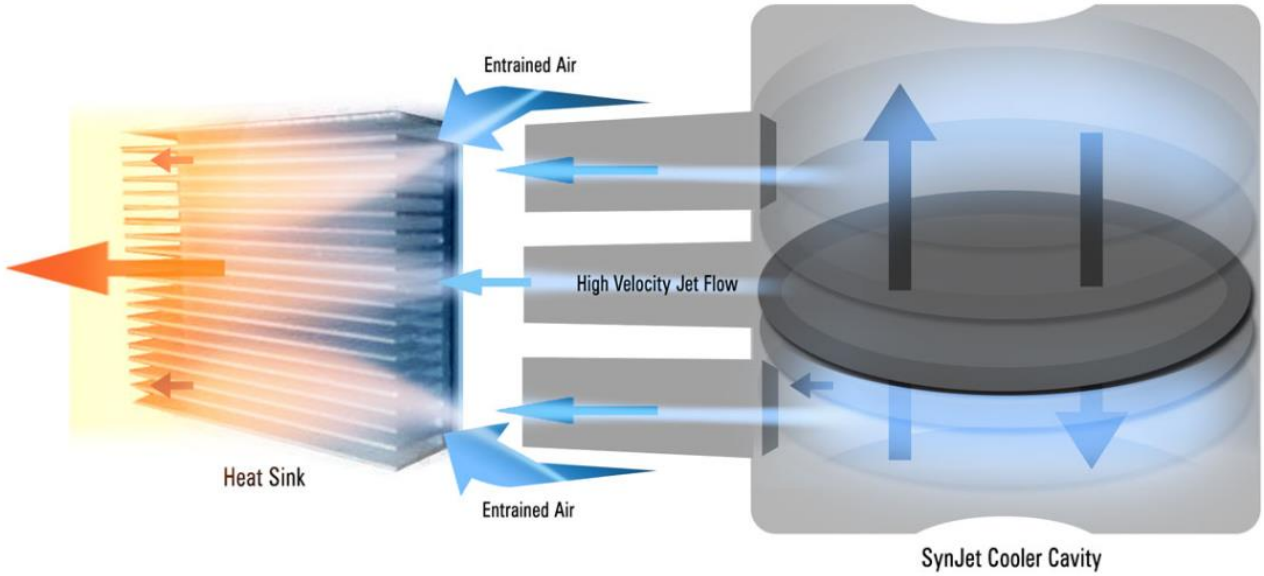

Figure 1.1 Models of zero-net mass-flux jets for cooling applications, developed by NuventixSinJet®. Retrieved from https://aircoolingpatariko.blogspot.com/2017/04/synthetic-jet-air-cooling.html, image link http://i.imgur.com/lPHKnZs.jpg?1?4497. Accessed 07 Jun 2018.

1.1 INTRODUCTION TO SYNTHETIC JETS

Internal fluids discharges into the environment have been widely studied historically, dealing to many powerful applications, as the infinite ones dealing with the usage of nozzles at any scale. In the particular case of a flow jet that is abruptly decelerated by the presence of a target surface it is conventional in literature to refer to an "impingement jet".
The know-how of synthetic jets, as well as many scientific productions, has been influenced and promoted a lot by the aerospace industry, as the chance to use a flow without a reservoir for it meets the tight design requirements of the field. Aerodynamic flow control applications have been recently developed thanks to synthetic jets, as for micro-air vehicles and unmanned air vehicles.

Jet impingement has been successfully implemented in various ind1ustrial processes, spreading from flow controlling to heat transfer enhancement. Remarkable developments have been reached especially in the aerospace industry, Although historically used for boundary layer control applications, in the last two decades there has been a great attention on the enhancement of natural and forced convection. Convection control and enhancement play a crucial role in many heating, cooling and drying applications. Between the most relevant and common there are: quenching and annealing of steels, textiles drying, glass tempering, the cooling of gas turbine blades and aircraft engine nacelles.

Around ten years ago the industry started to invest more on small-scale devices. The electronics industry found promising the theoretical and experimental investigation of those because of the new challenges on their markets. The increasing digitalization of most industrial processes, together with a constant growing demand of technological products for domestic applications, have two side effects: electronic circuits need to be more and more performing, but downsized, too. It means that high-density powered electronic circuits play a crucial role in most of the everyday human social activities.

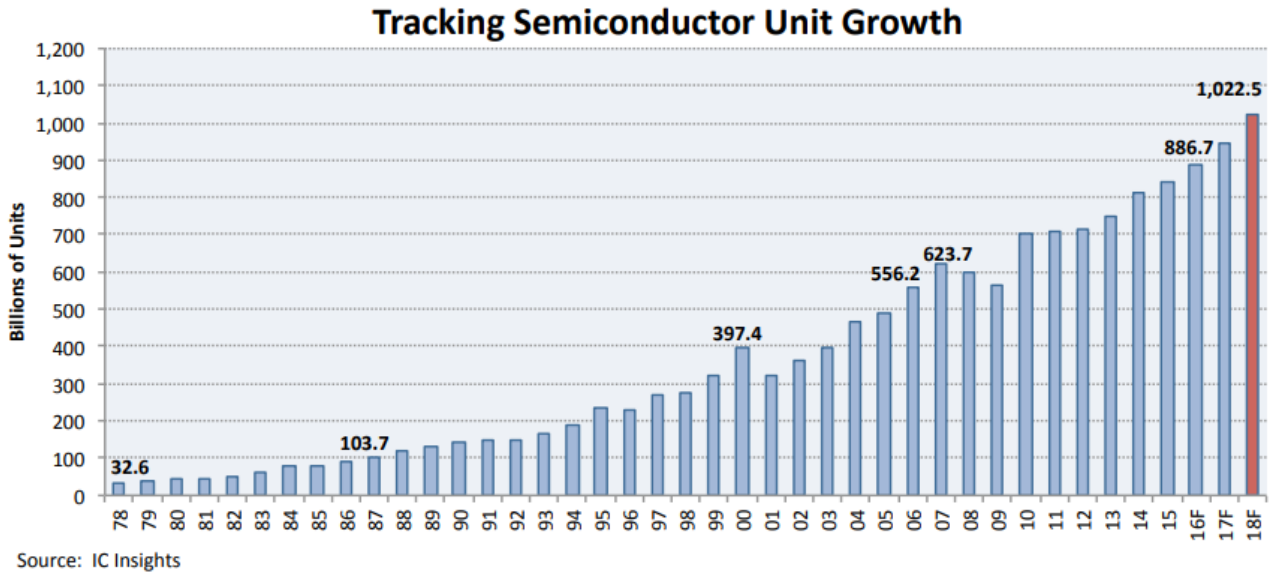

Figure 1.2 Semiconductor unit shipments per year, Research Bulletin March 7th, 2016, COPYRIGHT © 2016 by IC Insights,Inc.. Retrieved from http://www.icinsights.com/data/articles/documents/862.pdf. Accessed 07 Jun 2018.

The amount of energy they require is thus concentrated on small surfaces and the heat dissipated in the operative conditions is considerable. The high rates between the amount of heat wasted and the surface interested by the thermal exchange with the surroundings of the device become often a critical issue.

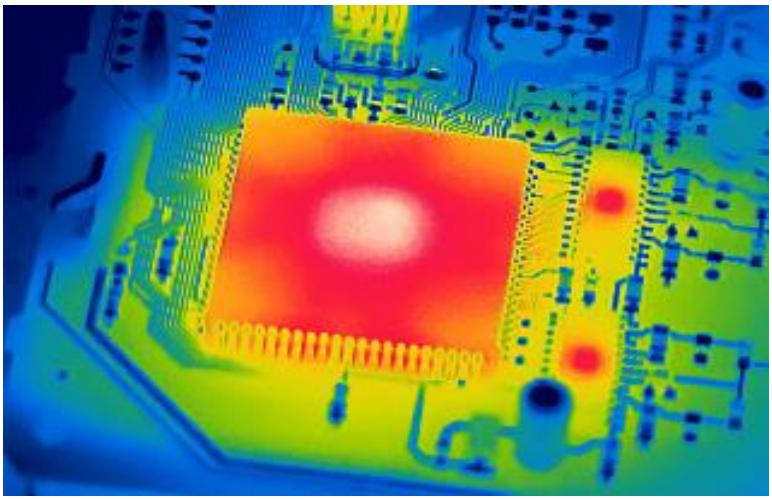

Figure 1.3 Excess heat causes efficiency losses and early product failures. Retrieved from https://www.digikey.com/en/articles/techzone/2013/jul/selecting-the-right-voltage-converter-is-not-just-about-peak-efficiency. Accessed 07 Jun 2018.

Both the life and the reliability of electronics components is dependent on their operating conditions, as humidity, dust and vibration. Nevertheless, none of the previous is as much crucial as the temperature. The conversion of energy from electrical to thermal, due to the dissipations, makes so that their temperature would tend to continuously increase, if a lack of thermal exchange with the environment occurred. In this case, the amount of heat stored by the electronic circuits exceeds the one released into the surroundings; consequently, the thermal level goes upon the suitable range of operating temperatures. Thermal stress significantly damages electronic components, dealing to their failure in most of the cases.

1.1.1 The value-added of synthetic jets

Synthetic jets create a turbulent jet by synthesizing the fluid in which they are embedded. Operating either on a macro or a meso-scale, synthetic jets are known as “zero-net-mass flux” devices: they generate a periodic pressure variation that does not add any mass to their surroundings, but rather momentum exchanges do occur. The periodic suction and blowing of working fluid is in fact so that the energy can be provided to the flow without adding extra mass.

Synthetic Jet Actuators (SJAs) operate in a stand-alone manner without any extra piping or fluidic packages (A. Glezer, 2002),meaning that there is no need for any hydraulic circuit nor fluid reservoir. It means that, by definition, they answer some of the new challenges in the electronics industry cooling scenario, as the need for downsizing and the easiness of fabrication and integration into a fluidic system.

- Schematically, synthetic jets consist of two main elements: an oscillating diaphragm and a cavity. Generally one side of the cavity retains the diaphragm, while the opposite one is the orifice region, that releases the jet. The periodic oscillation of the diaphragm is transmitted to the fluid in which it is embedded (most frequently air) so that it is intermittently induced in (suction phase) and expelled from the cavity (ejection phase).

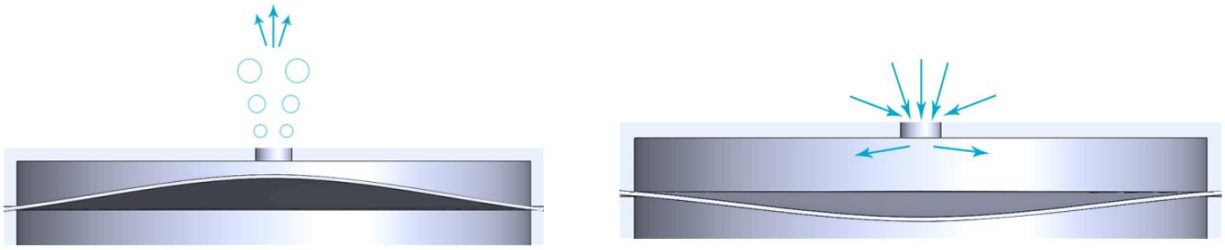

Figure 1.4 Synthetic jet working cycle, expulsion phase on the left, ingestion on the right. Drawing retrieved from https://blog.mide.com/synthetic-jets-basic-principles. Accessed 07 Jun 2018.

There are different types of jets, mainly depending on the configuration of the orifice region:

- *singular nozzle* versus *array of nozzles*;
- *circular nozzles* versus *rectangular nozzles*;
- *normal impingement on the target surface* versus *impingement at an angle*;
- *single phase* versus *two phases* (for liquid jets);
- *free* or *submerged* jets.

2| FUNDAMENTAL CONCEPTS

This section will be a summary for the key variables used in the analysis, as well as a mean to introduce the reader to the thermo-physical considerations from which the analysis output will be based.

2.1 ACOUSTIC WAVES

The importance of sound and its applications was firstly understood and recognized by Pythagora and his philosophical school, back in the 6th century BC, when the relationships between length, weight and height of vibrating ropes were investigated. Nevertheless, acoustics was considered a science only starting from the 17th century, when the development of modern mathematics tools allowed for an accurate description of the related phenomena. Galileo Galilei (1564-1642) provided the first relationships between length and frequency of vibrating strings. Many studies followed in the field, as the contribution given by Isaac Newton (1642-1727) in the "*Principia* (1687)", where there are important statements about the motion of waves in fluid; while D. Bernoulli (1700-1782), L. Euler (1707-1783) and G.L. Lagrange (1736-1813) focused on the vibration modes analysis.
The most important contribution came with J.-B. d'Alembert (1717-1783), who finally formulated the differential equation governing the motion of vibrating strings (1747):

$$\frac{\partial^2 u(x,t)}{\partial t^2} = c^2 \frac{\partial^2 u(x,t)}{\partial x^2} \tag{2.1}$$

or, equivalently, if the pressure is the dependent variable:

$$\frac{\partial^2 p(x,t)}{\partial x^2} = \frac{1}{c^2} \frac{\partial^2 p(x,t)}{\partial t^2} \tag{2.2}$$

Nowadays the "science of sound" represents a huge and complex branch of physics and engineering, dealing to what might be considered an infinity of real and potential applications. The high degree of non-linearity of the mathematics describing it complicates, sometimes significantly, the analysis of systems in which acoustic waves play a crucial role; that is, determine the effectiveness of the device under study.

Nevertheless, most acoustic phenomena determine very small perturbations of the medium that they go through, allowing for useful simplifications in many problems.

Being the usage of loudspeakers very common in everyday life applications, the implementation of simplifying models occurs frequently in literature and industrial applications.

In the last decades the proceedings in the industry and the constant refinement of research tools allowed for a proliferous production in the field of thermos-acoustics. The main subject of thermos-acoustics are the thermodynamics and fluid-mechanics processes taking places within sound waves, determining energy transformations.

Most of the processes convert acoustic energy to chemical or thermal, or simply the acoustic power is used to produce and/or transfer heat.

2.2 KEY TERMS

Hereby will follow a summary of all the relevant physical quantities playing a role in the processing and analyzing of the data.

2.2.1 Acoustics domain: key variables

The first crucial variable to be taken into account when it comes to acoustics wave is surely the wavelength, measured in meters and defined as:

$$\lambda = \frac{c}{f} \tag{2.3}$$

At the same time it is common to use in the field of acoustics the wavenumber, directly proportional to the inverse of the wavelength, it allows to compact the information within graphs with respect to the previous one. It becomes important when it comes to characterize the changes within the flow or the behavior of sound waves in the domain of the frequency (i.e. in defining their energy). Its unit is the reciprocal of the meter$[1/m]$.

$$K_{wn} = \frac{\omega}{c} = \frac{2\pi f}{c} \tag{2.4}$$

Being f [1/s] the frequency, T the temperature in Kelvin [K] and c [m/s] is the local speed of propagation of the sound wave, determined from equation:

$$c = 331.4\sqrt{\frac{T}{273}} \tag{2.5}$$

Information about the entity of the perturbation induced by the sound wave on the air particles is given by the Sound Pressure Level (SPL), measured in [dB] and defined as:

$$SPL = 20log_{10}\frac{p}{p_{ref}} \tag{2.6}$$

where Δp is the root-mean-square over time (a period) of the incremental change of pressure brought by the sound wave to the air, with respect to the static pressure, namely p_0. p_{ref} is the reference pressure with respect to which the logarithm is computed. A common value used for sound-level measurements is $p_{ref} = 2x10^{-5}Pa$, the same used in this work.

As with any mechanical wave, the transmission of sound highly depends on the medium that is passed through by acoustic waves. The quantity that allows for the evaluation of the perturbation induced by the wave in the medium is the characteristic impedance, $\rho_0 c$. Being the product between the density of the medium and the speed of sound through it, from the physical point of view it represents the ratio between the effective sound pressure and the effective particle velocity at any point crossed by a free plane sound wave.
In some applications as sound in enclosures it is really helpful to recur to energy-based approaches; particularly, the energy density is one of the most significant variables expressing the changes within the flow determined by sound waves. That is the power in Watt radiated per unit volume.

The energy density brought by a sound wave can generally be expressed as:

$$D(t) = \frac{1}{2}\left(\rho_0 u^2 + \frac{p^2}{\gamma P_0}\right) = D_{KE} + D_{PE} \tag{2.7}$$

While D_{KE} is the kinetic energy density imparted by the pressure differential to the flow, D_{PE} is the potential energy density, responsible for the small changes in volume of the gas. Both are measured in [W/ m^3].
By referring to an arbitrary control volume V_0 containing a mass m of air particles, with ρ_0 being the average density of those, it is possible to explicit these variables as follows,

$$D_{KE} = \frac{1}{2}\frac{mu^2}{V_0} \tag{2.7a}$$

$$D_{PE} = \frac{-\int p d\tau}{V_0} \tag{2.7b}$$

Where $d\tau$ is the incremental change in volume of the box. It must be noted that the integration constant for the above integral is set to zero, as there is no potential energy carried by a sound wave if there is no local change in pressure brought to

the air particles. Under the hypothesis of small changes in volume and substituting appropriately the variables according to the ideal gas law, it holds:

$$D_{PE} = \frac{1}{2}\frac{p^2}{\gamma P_0} \tag{2.7c}$$

Ideally for free progressive waves the two are equal in space, they both vary in time or space sinusoidally from zero to twice their mean value. For this reason it is appropriate to simplify the analysis by calculating the average energy density in a spherical free wave, as in most of low frequencies applications the dimension of the sound source can be modeled as a point source radiating spherical waves in the surroundings:

$$D_{avg} = \frac{p^2}{\rho_0 c}\left(1 + \frac{1}{2{K_{wn}}^2 r^2}\right) \tag{2.8}$$

The average energy density radiated by an acoustic source allows for the determination of the rms value in time of the air particles velocity:

$$u = \sqrt{\frac{D_{avg}}{\rho_0}} \tag{2.9}$$

2.2.2 Fluid mechanics domain: key variables

Hereby will follow a quick review about the main contributions in the analysis provided by the fluid mechanics domain, especially in terms of non-dimensional parameters, as they are precious to:

1) extend the analysis to other devices;
2) understand their physical meaning and extrapolate insights into the phenomena governing the flow.

A particular role in fluid dynamics is played by inertial forces, so that those become a very important term of comparison that could be used to scale the other forces playing a crucial role in the system under study. For this specific work, it is important to recall the importance of viscous, pressure and oscillating forces exerted on air by the alternation of a moving surface.
By comparing the magnitude of inertial to viscous forces, important information about the flow regime are provided by the Reynolds number, defined as:

$$Re = \frac{\rho u L}{\mu} \tag{2.10}$$

In the case of local pressure perturbations with respect to the static pressure, it is preferable to non-dimensionalize this variation by diving it for the dynamic pressure of the freestream flow. Such a ratio, called Euler number, represents the relative magnitude of pressure forces with respect to inertial forces:

$$Eu = \frac{p}{\frac{1}{2}\rho u^2} \tag{2.11}$$

In case of a periodic intermittent motion of air due to any oscillating force acting on it with a certain frequency, for example a loudspeaker membrane or a piezoelectric diaphragm, it is conventionally appropriate to study the flow regime through the Strouhal number, that provides the information about the changes of momentum within the freestream flow.

It is generally defined as:

$$St = \frac{fL}{u} \tag{2.12}$$

with:

f: frequency of the oscillations pulsating within the freestream flow;

L: characteristic length of the system, measured normally with respect to the flow streamlines;

u: freestream velocity of the flow.

For this set of non-dimensional parameters, the prediction of the velocity u is given by the calculations in the previous paragraph.

2.2.3 Heat and mass transfer: key variables

As the jet formation is governed by the Reynolds and the Strouhal numbers[27], a fully non-dimensional analysis was performed to investigate the relationships between the pulsating flow and the convection going onto the plate. It has been found that the most effective way to show those relations would be studying the Nusselt number as function of both the Reynolds and the Strouhal numbers.

The Nusselt number is hereby defined as:

$$Nu = \frac{qH}{k} \tag{2.13}$$

where:

H: height of the synthetic jet outlet section with respect to the target plate, [m];

k: thermal conductivity of air, [W/mK].

The variable q is defined as follows:

$$q = \frac{Q}{A(T_p - T_o)} \tag{2.14}$$

with:

Q = thermal power given to the target plate, [W];

A = area of the target plate exposed to the synthetic jet flow, [m^2;

T_p = mean temperature of the target plate, [°C];

T_o = air temperature at the outlet of the synthetic jet, [°C].

The definition itself of synthetic jets as "zero-net-mass-flux principle" devices immediately recalls the importance of evaluating the exchanges in momentum within the flow, being their principal value-added. On the other side, this investigation main purpose is to bring insights about the heat and mass transfer phenomena occurring within them. It turns out by principle that a non-dimensional parameter within the thermos-physics domain has to be introduced as well, the so-called Prandtl number.

$$Pr = \frac{\nu}{\alpha} = \frac{\mu c_p}{k} \tag{2.15}$$

where:

ν = kinematic viscosity or momentum diffusivity, [Ns/m^2];

α = thermal diffusivity or coefficient of temperature exchange, [m^2/s;

c_p= specific heat at constant pressure, [J/kgK];

It is also appropriate to recall the definition of thermal wave number, which will allow us to infer some consideration in the section dedicated to data analysis:

$$K_\alpha = (1+j)\sqrt{\frac{\gamma\omega}{2\alpha}} \tag{2.16}$$

More precisely, for air at 18 °C and a pressure of 760 mmHg it becomes $K_\alpha = 1.602(1+j)\sqrt{\omega}^{-1}$, with j being the imaginary unit

2.2.4 Heat and mass transfer within sound waves in the audible range

Most of the sound waves in the audible range can be modeled through simplifying hypothesis that do not affect the accuracy of the analysis.

In the case of ideal gases, most commonly air, the particles of the gas:

1) have a negligible volume with respect to the one occupied by the gas;
2) are subject to elastic, instantaneous and random collisions, whose effects are negligible as well;
3) have an intermolecular spacing of the order of 10^{-9} m.

It is possible to retrieve in literature calculations about the speed of a thermal diffusion wave, whose velocity is small compared to a compressional wave, travelling at the speed of sound. Particularly, with air having a dynamic viscosity around 1000 cps, it is possible to determine a 0.5 m/s velocity for the first one. It turns out that the distance travelled by this one is very small compared to the one travelled by a sound wave. Furthermore, in the audible range of frequencies those distances are higher with respect to the intermolecular spacing of air molecules (around three order of magnitudes on average) , it becomes intuitive to infer that the heat transfer within sound waves in such conditions is negligible. The sound waves in those applications could be modeled as adiabatic, meaning that in the case of this system the enhancement of natural convection happens essentially to the extend that the new fluid is renewed over the plate, subsequently the higher thermal gradient in the fluid over the plate changes enhances heat transfer within the boundary layer.

3| *INSTRUMENTATION*

The following section will provide all the necessary information related to all the components belonging to the setup and the main devices that contributed to the assembly of the system.

3.1 THE EQUIPMENT

The first focus will be on the components allowing for the execution of the experience, to provide a first idea for both the fluid dynamics and thermodynamics phenomena that are related to the synthetic jet.

3.1.1 The loudspeaker

The loudspeaker represents the core of the synthetic jet. Being its vibrations responsible for the exchanges in momentum characterizing the synthetic jet, it will be referred to as the *diaphragm*.

Figure 3.1 Visaton® FRS 8 full-range driver. Copyright© 2017 VISATON GmbH & Co. KG.Retrieved from*http://www.visaton.de/en/products/fullrange-systems/frs-8-4-ohm*. Accessed 07 Jun 2018.

Specifically, the loudspeaker adopted in the setup is a Visaton® FRS 8 full-range driver. It allowed the execution of all the tests performed during the experience, as no failure nor damage was ever observed.

Table 3.1 Technical data of the Visaton® FRS 8 full-range driver. Courtesy of VISATON® GmbH & Co.

TECHNICAL DATA			
Rated power	*30 W*	Maximum power	*50 W*
Nominal impedance Z	*4 Ohm*	Frequency response	*100-20000 Hz*
Mean sound pressure level	*82 dB (1 W/1 m)*	Opening angle (-6 dB)	*180°/4000 Hz*
Excursion limit	*+/2,5 mm*	Resonance frequency fs	*120 Hz*
Magnetic induction	*0,8 T*	Magnetic flux	*200 µWb*
Front pole-plate height	*4 mm*	Voice coil diameter	*20 mm*
Height of winding	*4,5 mm*	Cutout diameter	*73 mm*
Net weight	*0,28 kg*	D. C. resistance Rdc	*3,5 Ohm*
Mechanical Q factor Qms	*3,61*	Electrical Q factor Qes	*0,85*
Total Q factor Qts	*0,69*	Equivalent volume Vas	*11*
Effective piston area Sd	*31 cm²*	Dynamically moved mass	*2,5 g*
Force factor Bxl	*2,2 T m*	Inductance of the voice coil L	*0,4 mH*
Connections	*4,8 x 0,8 mm (+) 2,8 x 0,8 mm ()*	Temperature range	*25 ... 70 °C*

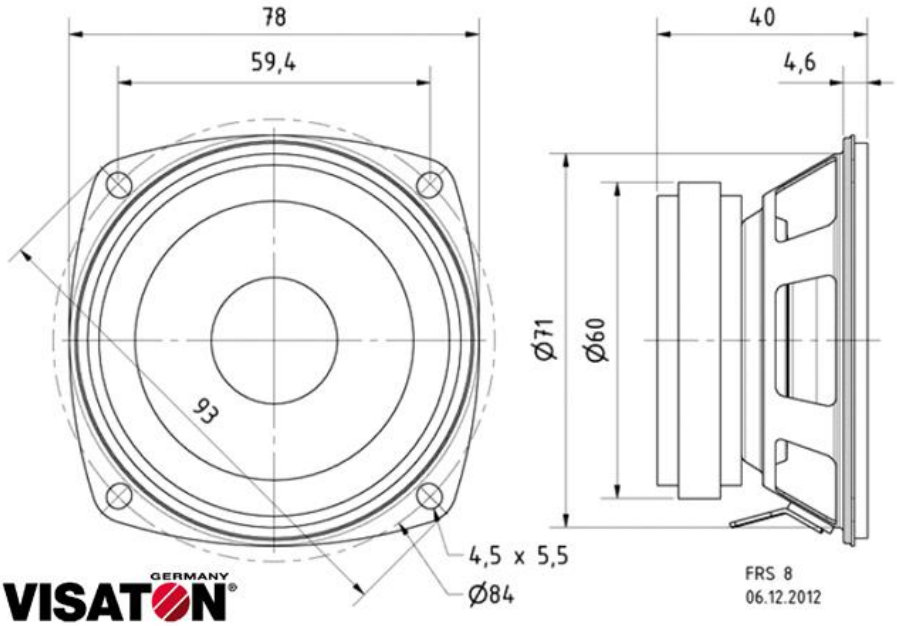

Figure 3.2 Visaton® FRS 8 full-range driver sketch together with the main dimensions. Copyright © 2017 VISATON® GmbH & Co. KG. Retrieved from *http://www.visaton.de/en/products/fullrange-systems/frs-8-4-ohm*. Accessed 07 Jun 2018.

3.1.2 Plate adjustment unit

The plate adjustment unit consists of two slides, rack and pinion assemblies, designed by Misumi Corporation© for high precision applications.

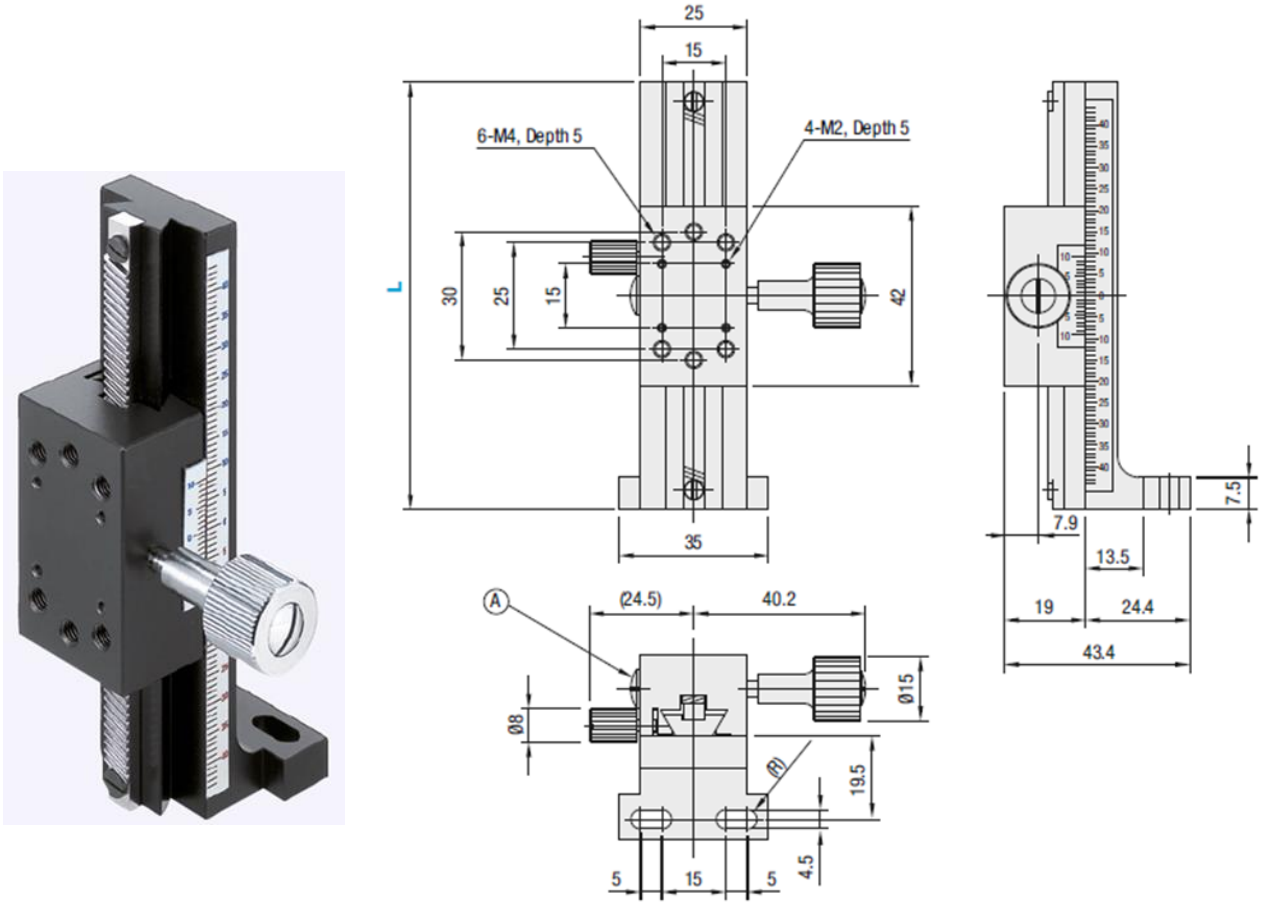

Figure 3.3 Misumi Corporation© [High Precision] Z-Axis Dovetail Slide, Rack & Pinion ZLWG50 and relative dimensions. Retrieved from*https://uk.misumi-ec.com/pdf/fa/2014/P1_1955-1956_F28_EN.pdf*. Accessed 08 Jun 2018.

Table 3.2 Misumi© [High Precision] Z-Axis Dovetail Slide, Rack & Pinion ZLWG50 technical specifications. Courtesy of Misumi Corporation©.

Part number	*ZLWG50*
L (see fig. 7)	*50 mm*
Travel distance	*±15 mm*
Travel per rotation	*18 mm*
Load capacity	*14,7 N*
Travel accuracy (Straightness)	*30 µm*
Weight	*0,120 kg*

Two L-shaped bars have been mounted on both the slides, symmetrically with respect to the their longitudinal axis (front view, fig.). The bars allow for the clamping of the plate holder, by screwing through-polymeric-bolts, concentric to the plate holder positioning holes.

3.1.3 Power supply

The power supplied to the heaters is provided by a precision laboratory DC power supply model PL310QMT, manufactured by ThurlbyThandar Instruments Ltd.

Figure 3.4 DC power supply model PL310QMT, ThurlbyThandar Instruments Ltd. Retrieved from *http://www.ebay.co.uk/cln/tony_ling/test-equipment/105211509011*. Accessed 08 Jun 2018.

Table 3.3 DC power supply model PL310QMTtechnical specifications. Courtesy ofThurlbyThandar Instruments Ltd.

GENERAL	
Power supply (AC 50/60Hz)	*110, 120, 220 or 240V±10%*
Size	*170x 425x 265mm(H x W x D)*
Electrical Safety	*IEC348, IEC1010-1*
Operating Range	*5°C to 40°C, 20% to 80% RH*
Weight	*11.5 kg*
EMC	*EN50081–1 , EN50082–1*
MAIN OUTPUT(S)	
Output Range	*0 - 32 Volts nominal; 0 - 1.1A*
Voltage Setting	*By coarse and fine controls; resolution <5mV*
Current Setting	*By single logarithmic control*
Output Mode	*Constant voltage (or current) mode (automatic cross-over)*
Configuration	*Isolated, True parallel, Series or Series Tracking*
Selection	*via front panel switches*
Output Switch	*Isolates the output. Permits voltage and current limits to be set up before connecting the load*
Output Terminals	*4 mm terminals on 19 mm spacing*
Output Impedance	*Constant Voltage: Typically <5mΩ at 1kHz* *Constant Current: Typically 50kΩ*
Output Protection	*Max. output voltage+20volts forward; diode clampedfor reverse, upto3Areversecurrent*
Load Regulation	*<0.01%of max. output for 90%load change*

Line Regulation	*<0.01%of max. output for 10%line change*
Remote Sense	*Eliminates up to 0.5Vdrop per lead*
Ripple and Noise	*Typically <1mVrms*
Transient Response	*<20 µsec to <50mVfor 90%load change*
Temperature Coefficient	*Typically <100ppm/°C*
Meter Type	*Dual 4 digit with 12.5mm LEDS* *Reading rate 4 per second*
Meter Resolution	*Voltage: 10mVover the entire range* *Current: 1mAover the entire range*
Meter Accuracy	*Voltage: ±(0.1%of reading + 1 digit)* *Current: ±(0.3%of reading + 1 digit)*
Current Meter Damping	*Nominally 20ms switchable to 2 sec for averaging of rapidly varying loads*
LOGIC OUTPUT - PL310QMT	
Output	*Fixed 5V± 0×1Vat >1.5A*
Output Protection	*Forward up to 16V, Reverse up to 3A*
Load Regulation	*< 0×3%for 50%load change*
Line Regulation	*< 0×1%for 10%line change*

3.2 MEASURING INSTRUMENTS

Hereby not only the instruments measuring the different variables will be treated, but great attention will be addressed to the devices that allow for the both the set and the monitoring of the test experimental parameters.

3.2.1 Displacement sensor

The loudspeaker membrane displacement is measured through a CCD Laser Displacement Sensor LK-G15, manufactured by Keyence Corporation© for super-precision applications.

Table 3.4 CCD Laser Displacement Sensor LK-G15 technical specifications. Courtesy ofKeyence Corporation©.

Sensor head specification		
Model		*LK-G15*
Reference distance		*10 mm*
Measuring range		*±1 mm*
Light source		*Red semiconductor laser*
	Wavelength	*650 nm (visible light), Class II (FDA)*
	Output	*0.3 mW max.*
Spot diameter (at reference distance)		*Approx.20 x 500 µm*

Linearity		*±0.03% of F.S. (F.S.= ±1 mm)*
Repeatability		*0.02 µm (0.01 µm)*
Sampling frequency		*20/50/100/200/500/1000 µs (Selectable from 6 levels)*
LED display		*Near the center of the measurement: Green lights* *Within the measurement area: Orange lights* *Outside the measurement area: Orange flashing*
Temperature characteristics		*0.01% of F.S./°C (F.S.= ±1 mm)*
Environ-mental resistance	Protective construction	*IP67 (IEC60529)*
	Ambient luminance	*Incandescent/fluorescent lamp:10000 lux max.*
	Ambient temperature	*0 to +50°C, No condensation*
	Relative humidity	*35 to 85%, No condensation*
	Resistance to vibrations	*10 to 55 Hz, multiple amplitude 1.5 mm; 2 hours in each direction of X, Y, and Z*
Material		*Aluminum die-cast*
Weight (including the cable)		*Approx. 190 g*

3.2.2 Waveform generator

The signal sent to the loudspeaker is a low-distorsion sine wave synthesized with direct digital techniques by an Agilent Technologies 33120A Function/Arbitrary Waveform Generator. Having a 12-bit resolution and a sampling rate of 40 MSa/s, the 33120A is able to generate accurate standard waveforms with uncompromising performances.

Table 3.5 Agilent Technologies 33120A Waveform Generator technical specifications. © Agilent Technologies, Inc. 2001, 2004, 5968-0125EN.

GENERAL			
Power Supply	*110V/120V/220V/ 240V ±10%*	Power Line Frequency	*45 Hz to 66 Hz, 360 Hz to 440 Hz*
Power Consumption	*50VA peak (28 W average)*	Operating Environment	*0°C to 55°C*
Storage Environment	*-40°C to 70°C*	Interface	*IEEE-488 and RS-232 standard*
Language	*SCPI - 1993, IEEE-488.2*	Dimensions (W x H x D)	*Bench top* *254mm x 104mm x 374mm* *Rack mount* *213mm x 89mm x 348mm*
Weight	*4 kg*	Vibration and Shock	*MIL-T-28800, Type III, Class 5*

Acoustic Noise *30 dBa*	Warm-up Time *1 hour*
SYSTEM CHARACTERISTICS (Configuration Times)	
Frequency Change *30 ms*	Amplitude Change *30 ms*

The front panel of the generator is intuitive and straightforward to use, as a simple key press allows to access the frequency and the amplitude functions, through two different buttons respectively labeled "Freq" and "Ampl". A comfortable knob is used to adjust their values without too much distraction, as it is located right next to the display. The voltage is set in V_{p-p}.

Table 3.6 Wafeforms characteristics produced by the Agilent Technologies 33120A Waveform Generator. © Agilent Technologies, Inc. 2001, 2004, 5968-0125EN.

WAVEFORMS AND FREQUENCY CHARACTERISTICS			
Standard	*Sine,square,triangle,ramp,noise, sin(x)/x,ex-ponential, rise expon-ential fall, cardiac,dc volts.*	Waveform length	*8 to 16,000 points*
Sine and square waves	*100 µHz - 15 MHz*	Resolution	*10 µHz or 10 digits*
Accuracy	*20 ppm in 1 year, 18°C - 28°C*	Temperature Coefficient	*< 2 ppm/°C*
SINEWAVE SPECTRAL PURITY			
Harmonic distortion	*-70 dBc (dc to 20 kHz)*	Total harmonic distortion	*<0.04% (dc to 20 kHz)*
OUTPUT CHARACTERISTICS			
Amplitude (into 50Ω)	*50 mVpp - 10 Vpp*	Accuracy (at 1 kHz)	*± 1% of specified output*
Flatness (sinewave relative to1kHz)	*± 1% (0.1 dB) (< 100 kHz)*	Operating Environment	*0°C to 55°C*
Output Impedance	*50Ω (fixed)*	Resolution	*3 digits, amplitude and offset*

3.2.3 Thermocouple module

A 16-channels thermocouple input module was used for temperature data acquisition. The manufacturer, National Instruments Corporation©, an excellence in the scientific domain of laboratory measuring instruments, provides the LabVIEW environment. It allows to monitor in real time the measured temperatures, eventually writing those variables on a text file. The model, NI 9213, has the following specifications (see Table 7):

Table 3.7 Thermocouple input module NI 9213 specifications. Copyright © 2012 National Instruments corporation.

GENERAL	
Operating system/target	*Real-time, Windows*
Measurement type	*Temperature, Thermocouple*
Signal conditioning	*Open thermocouple, Cold-junction compensation*
ANALOG INPUT	
Differential channels	*16*
Resolution	*24 bits*
Sample rate	*1200 S/s*
Bandwidth	*78 Hz*
Maximum voltage range	*-78.125 mV, 78.125 mV*
Simultaneous sampling	*No*
PHYSICAL SPECIFICATIONS	
Length	*88.11 mm*
Width	*22.86 mm*
I/O connector	*36-position spring terminal*
Minimum Operating Temperature	*-40 °C*
Maximum Operating Temperature	*70 °C*
Minimum Storage Temperature	*-40 °C*
Maximum Storage Temperature	*85 °C*

3.3 ADDITIVE MANUFACTURING TECHNOLOGY

A brief make-or-buy decision phase anticipated the experimental setup assembly. The usage of a 3D printer was not brought in during the design process to answer specific problematic; rather, it was considered a necessary complement to the whole design and assembling process, since the first phases. The time available for the experimental work, the need to build up a non-preexisting setup for it and the course of the whole experience confirmed this first guess.

3.3.1 3D printing technology

A 3D printer was used to either prototype or build-up the setup accessories whose design needed to be changed and tested in an ongoing short-term process.

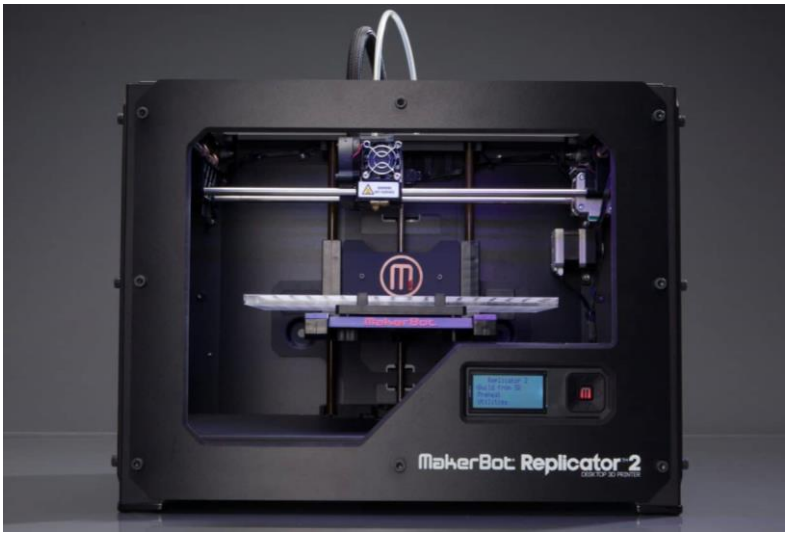

Figure 3.5 3D printer MakerBot Replicator2™. Retrieved *from https://www.makerbot.com/media-center/2012/09/19/a-whole-new-makerbot-introducing-replicator-2-desktop-3d-printer*. Accessed 08 Jun 2018.

The device used was a MakerBot Replicator2™, a desktop 3D printer for laboratory applications manufactured by MakerBot®.

Table 3.8 MakerBot Replicator2™ specifications. Courtesy of MakerBot™.

PRINTING			
Print Technology	*Fused Filament Fabrication*	Build Volume	*285 x153x155 mm (LxWxH)*
Layer Resolution Settings	*High 100 microns* *Standard 200 microns* *Low 300 microns*	Positioning Precision	*XY: 11 microns* *Z: 2.5 microns*
Filament Diameter	*1.75 mm*	Nozzle Diameter	*0.4 mm*
PHYSICAL DIMENSIONS			
Without Spool	*490 x 320 x 380 mm*	With Spool	*490x 420 x 380 mm*
Weight	*11.5 kg*	Shipping Weight	*20.2 kg*
TEMPERATURE			
Operating Ambient	*15° – 32° C*	Storage	*0° – 32° C*
SOFTWARE			
Software Bundle	*MakerBotMakerWare™*	File Types	*.stl, .obj, .thing*

ELECTRICAL			
AC Input	*100 – 240 V, ~2 amps, 50 – 60 Hz*	Power Requirements	*24 V DC @ 6.25 amps*
Connectivity	*USB, SD card [FAT 16, max. 2GB]*		
MECHANICAL			
Chassis	*Powder-coated steel*	Body	*PVC Panels*
Build Platform	*Acrylic*	XYZ Bearings	*Wear-resistant, oil-infused bronze*
Stepper Motors	*1.8° step angle with 1/16 micro-stepping*		

4 | THE EXPERIMENTAL SETUP

The whole experimental setup has been assembled on-purpose for this thesis work. Some of the components have been designed by the author of this thesis. Others needed to be machined to fit in the whole system design.

The 3D printer was adopted to create the different nozzles reducing the synthetic jet cavity diameter and the target plate supports. As metal components would have been sent necessarily to an external contractor for manufacturing, this option was guessed to be the most convenient and less time-consuming in the make-or-buy decision preliminary process. So it was proved to be.

4.1 PROTOTYPING THE SETUP

Before defining the protocol of the experiments, a preliminary phase was needed in order to design and build-up the setup to fulfill the experimentation aims.

During the preliminary tests the whole setup was functional, even though it lacked various improvements. The loudspeaker was bolded to a single cylinder, representing the cavity of the synthetic jet.

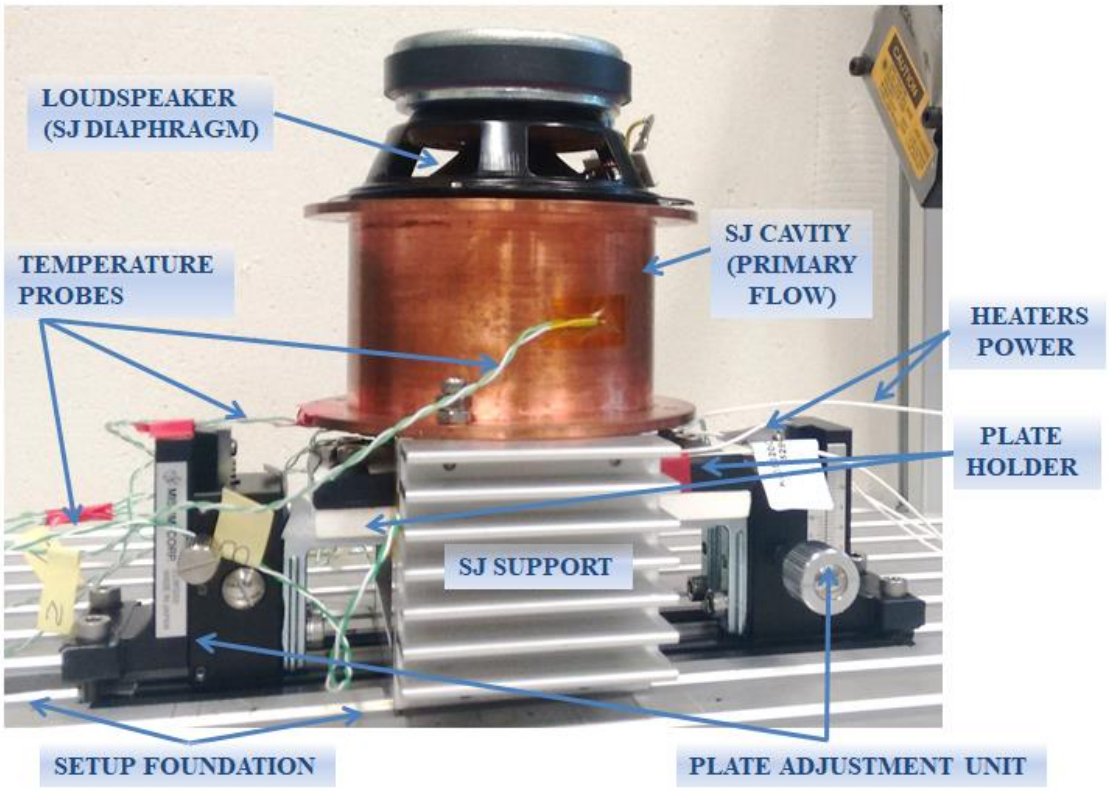

Figure 4.1 First setup prototype. Courtesy of Agency for Science, Technology and Research (A*STAR).

The main purpose of the first setup was checking connections and verifying the synthetic jet operativity. The target plate was hold between two tablets properly machined from poor ceramic material in order to be bolted to the plate adjustment unit. This plate was found to be too small to fully exploit the synthetic jet power, as the whole cavity outlet section was greater than its thermal exchange surface.

The first prototype of the system included a very simple support for the synthetic jet: an aluminum u-shaped beam with the two external finned surfaces.

4.2 MANUFACTURED COMPONENTS

A support for the target plate was needed and manufactured in A*STAR laboratories, in order to hold it tight to the plate adjustment unit. This last one allows then the repositioning with respect to the outlet of the synthetic jet. The support needed a quick design study and a few prototypes were built before getting its final shape.

Differently, the design of the nozzles was found to be straightforward and each of those was slightly modified to fit at the best the cavity hosting them. Three different synthetic jets diameters have been extruded through the 3D printer and subsequently tested: 25, 12.5 and 6 mm respectively.

4.2.1 Design of the plate holder

During the preliminary tests, it was found that the ceramic support was too brittle for the purpose, as any readjustment of the plate unit could unexpectedly scrape or crack it. Some ordinary insulating tape has been stick around its volume as, it could prevent it from flaking and damaging. The same tape was used on the foundation and on the Misumi clampers bolted on it, to prevent direct metal to metal contact; thus, the resulting level of vibrations and noise. Both the vibrations and the intermittent jet action made so that ceramic powder was frequently found on the plate. At this first point only the heaters were attached to the plate, but obviously the temperature probes would have suffered the presence of dust, too. Thus, an additive manufacturing technology seemed to be the solution to easily overcome those drawbacks.

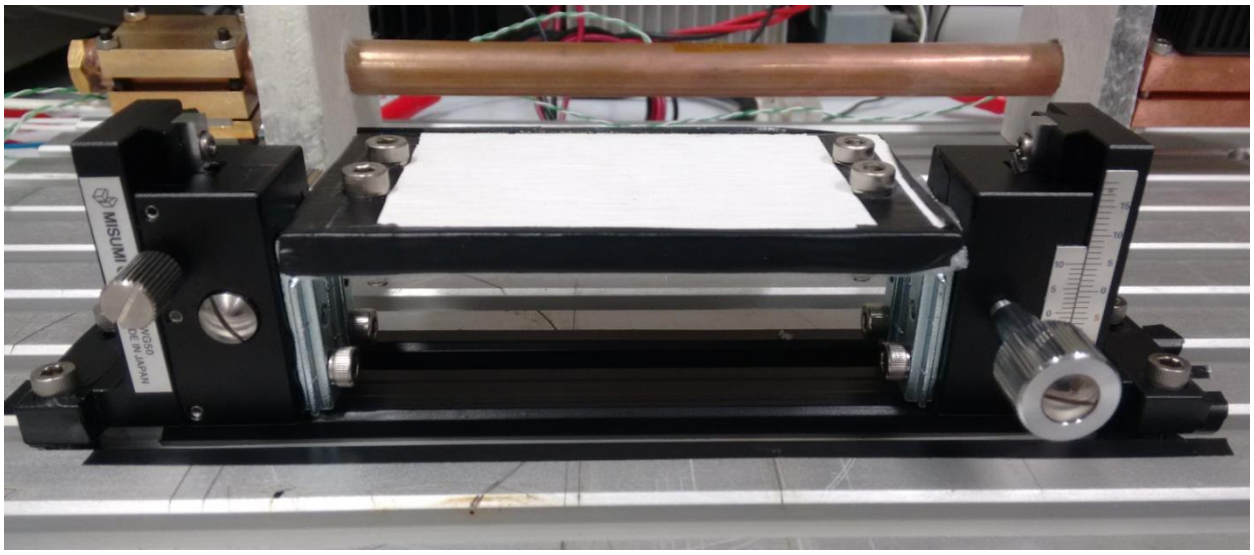

Figura 4.2 First prototype for the plate holder, made in ceramics material locally manifactured by the author of this thesis at A*STAR facilities. Courtesy of Agency for Science, Technology and Research (A*STAR)

A new target plate was ordered, but in the meanwhile a quick feasibility study was improvised to test the idea. A first poly(lactic acid) (PLA) plate support was built through the 3D printer to host the smaller plate (fig.11a)).

As the power connection terminals of the heaters are delicate and quite stiff, they could not bend completely freely once stuck to the target plate without compromising the adhesion of the heaters on the plate or, worst case, damaging. Thus, the lower part of the first PLA plate holder hosts two slots to properly set in place the hea

ers and their connections. Height through holes were extracted from it to make so that the temperature probes could be inserted from the bottom, allowing for different configurations. The upper part was designed so that most of the plate surface could be exposed to the jet, by clamping and framing the plate by a couple of millimeters on each of the four sides. Both the parts have four holes to host the through pins that clamp together the plate and secure the plate holder assembly to the plate adjustment unit.

In the design phase the holes were made small (Ø3 mm) so that they could host the temperature probes terminals with the lowest clearance possible. Only the tip of the sensor was put in contact with the plate, to affect at the least the measurements and the heat transfer through the plate itself. Unfortunately, while assembling, it was noticed that the stiffness of the cables and the small dimensions of the plate made such a positioning difficult and time-consuming. During the first tests it was also noticed that vibrations could easily detach the probes from the plate.

A thermal adhesive tape was used to stick the probes on the plate. It also meant that the terminals of the probes were folded between the lower part of the plate holder and the plate itself. As more space was required to host each of the probes on the plate by such positioning, it resulted unnecessary to design as many holes as before to allow for their positioning in different configurations. It also meant that the number of measuring points for the temperature on the plate had a major constraint and the analysis of the heat transfer going through the plate itself was thus compromised.

At the same time such positioning proved to be resistant to vibrations and different operating conditions, as they were never found out of place during the data collection. More important, it avoided the risk to get the boundary layer temperature in the proximities of the plate or, worst, the temperature of the air pulsating locally around the plate, affecting in sensible way the accuracy of the calculations related to the convection around the plate.

As soon as the final target plate (101 x 97 mm) could be set in place, a similar plate holder was built up, too.At this time only six holes were placed for the sake of the temperature measurements, due to the just above mentioned reasons.

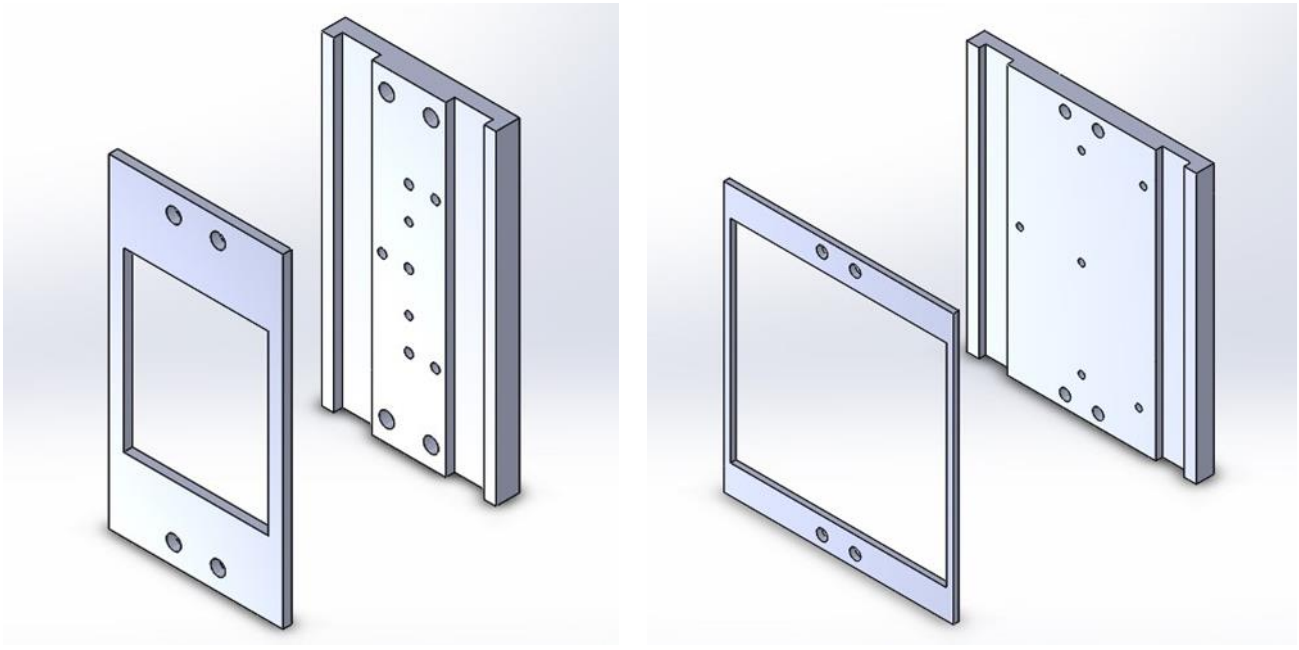

a) b)

Figure 4.3 Target plate holder no. 1 and 2, respectively in a) and b). Courtesy of Agency for Science, Technology and Research (A*STAR).

During the following tests it was observed that the heat conduction through the plate holder was not negligible, as the bars used to fix the plate on its adjustment unit were considerably warm, reaching almost 40°C if the heaters were left on and the synthetic jet was off.

A quick investigation on the thermomechanical properties of PLA composites [2]revealed that thermal conductivities values are around 0.25 W/m·K, one order of magnitude higher than the range of values for thermal conductivity of the air in the experimental conditions. Additionally, it was also found that PLA is not thermally stable and has a glass transition temperature around 55°C . Before turning on the jet, at regime, the plate temperature was likely to be more than 70°C. After a few thermal cycles PLA properties can vary sensibly, including its degree of crystallization. It meant that after a few tests thermal degradation effects were observed on the plate holder, whose surfaces were not completely flat anymore.

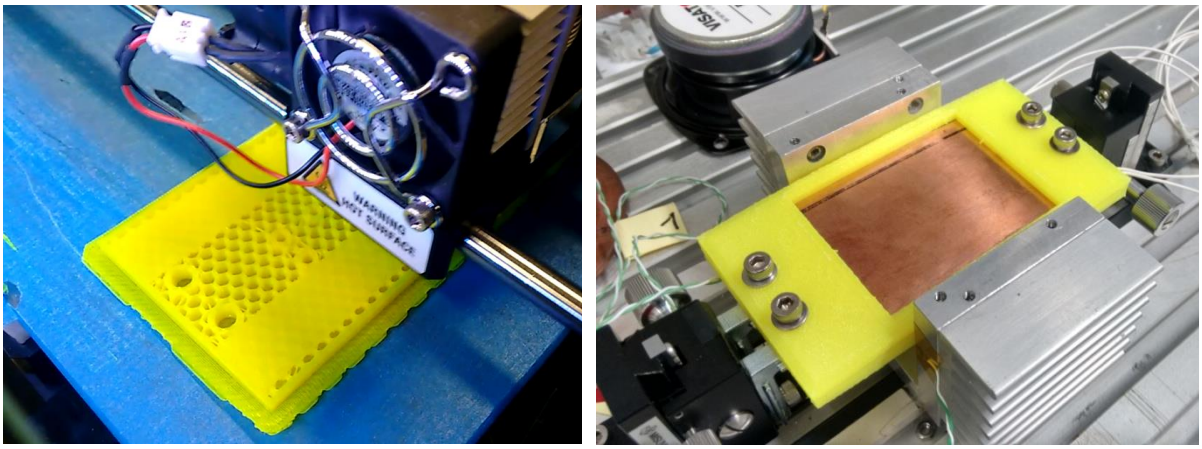

Figura 4.4 Extrusion process for the plate older no. 1 and relative assemblance. Courtesy of Agency for Science, Technology and Research (A*STAR).

It would have been hard and time-consuming to shape a plate holder with different techniques and/or materials; furthermore, new unexpected problems could have arise once mounted. The best compromise looked to be simply a downsizing of the plate holder. One more prototype was built in the shape of rather a frame for the target plate, just by bordering each of its sides by approximately 2 mm of PLA, obtained by simply clamping the plate through the holders. Approximately all the plate surface resulted exposed to air; in such a way convection resulted to be the dominant heat transfer mechanism. This last condition is fundamental for the sake of the whole analysis.

Two additional tiny holes were located on both the sides of the holders, to make so that two through pins could clamp tight the plate between the two parts, preventing from an excess of deformation that could not allow it to lie horizontally. One slot for each part was located to allow the passage of the cables respectively belonging to the temperature probes and the heaters. This last model suffered minor losses, as a temperature reduction of the support bars was observed. At the same time the lower amount of material used for the extrusion

made so that it more likely deform. Furthermore, it was noticed that the interaction between the internal reactions of the PLA on thermal stress and the compression force exerted by the through pins further deformed the structure anisotropically.

This result was seen as an improvement with respect to the previous ones, especially from the heat transfer standpoint. Nevertheless, it was difficult to maintain the plate flat, as the deformation of the holders bended it slightly on both the sides. Thus, it was necessary to go back to the design process.

Figure 4.5 Target plate holder no. 3. Courtesy of Agency for Science, Technology and Research (A*STAR).

Subsequently, the final support was successfully designed, in the shape of a couple of small tweezers clamping together the plate on four small symmetrical spots, on the two sides respectively, guaranteeing its flatness during operation. By reducing enormously the amount of material in contact with the plate and leaving most of it exposed to air it was observed that:

- no significant deformation was found after many tests (thus, thermal cycles);
- the plate perfectly lied horizontally, clamped on four points, with no significant pressure exerted by the structural changes of the PLA;
- the temperature of the bars in the plate adjustment unit lowered significantly, up to a couple of degrees higher than the ambient one, making so that the heat losses due to conduction through the plate support bars could be neglected for the sake of the whole analysis.

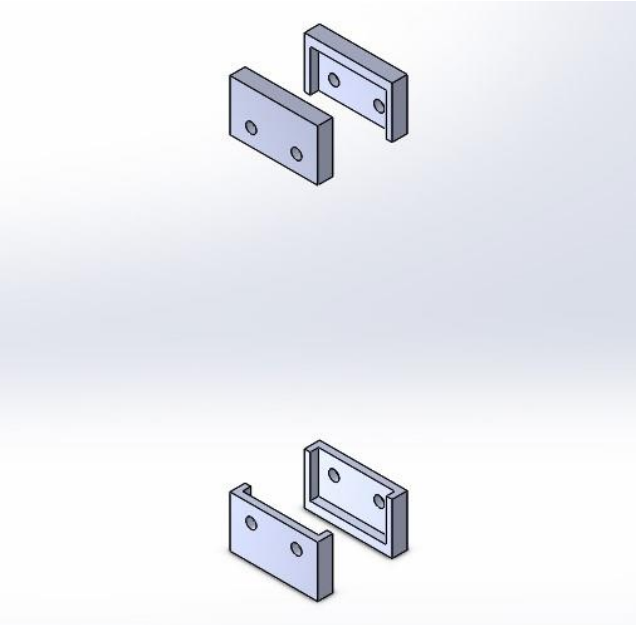

Figure 4.6 Final design for the target plate holder. Courtesy of Agency for Science, Technology and Research (A*STAR).

4.2.2 Design of the nozzles

Different studies available in literature highlighted the dependence of synthetic jets performances on different design and operating parameters. Between the design parameters a major role is assumed by the so-called nozzle-to-spacing ratio, H/d_{sj}, where:

d_{sj}: diameter of the synthetic jet at the outlet of the nozzle;

H: vertical distance between the outlet of the nozzle and the plate.

Since the setup available did not allow to extrapolate many considerations out of the second variable, it was chosen to discuss the influence of the nozzle-to-space ratio by rather changing the nozzle diameter. The preliminary tests showed that the efficiency of the jet simply increased by nearing the plate to the outlet of the cavity, as intuition suggested. In order to further investigate the height as a determining variable in the analysis it would have been optimal to use a different driver as diaphragm; the best option would have been a piezoelectric diaphragm. Both the time and the resources for this experience did not allow the implementation of such improvement: it would have required a redesign of the full setup, plus the times related to the manufacturing and testing. This last scenario was definitely considered counterproductive for the sake of the whole analysis.

As the improvement of the design was within the main aims of the experience, with a special regard towards the improvements in terms of performances, it was found appropriate to work with the plate as close as possible to the cavity, in accordance with the available power of the driver.

On the other hand, it was soon noticed that the cavity of the synthetic jet could farther be restrained, to accelerate the flow going onto the plate. Since machining other components would have needed longer manufacturing times, it was found appropriate to implement the 3D printer for this purpose. In fact, the most practical solution was to extrude accessories that could be inserted inside the cavity, restraining it with the lowest minor losses of the case.

Particularly, it was avoided a sudden change in area inside the cavity by building converging *nozzles* that could guide the flow up to the outlet section of the cavity. The first one was built with a 50 mm outlet diameter, almost one third of the cavity diameter, to make sure there would have been a sensible change in behavior of the jet. The following ones were dimensioned by halving the 50 mm diameter two times, respectively 25 and 12 mm, with the guess that this choice could deal to any particular conclusion.

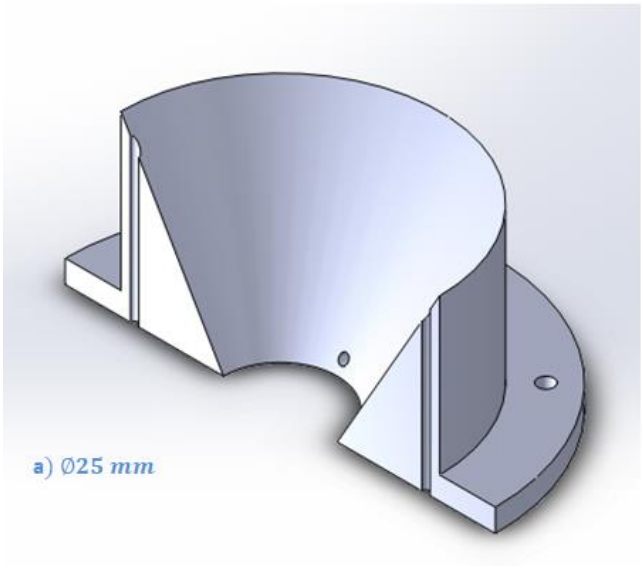

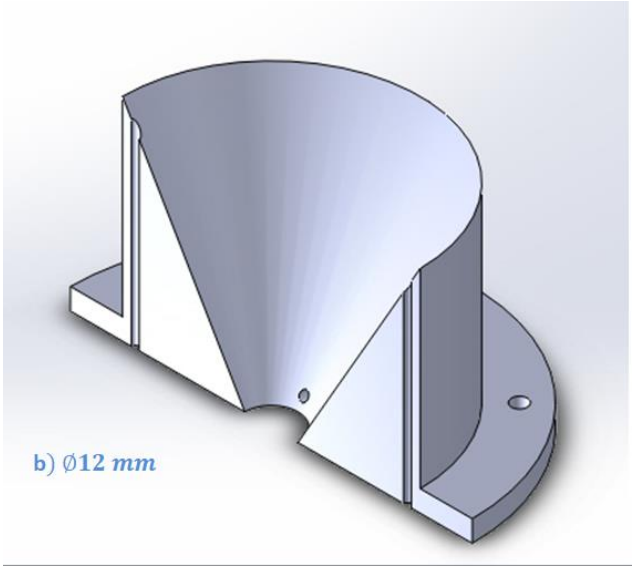

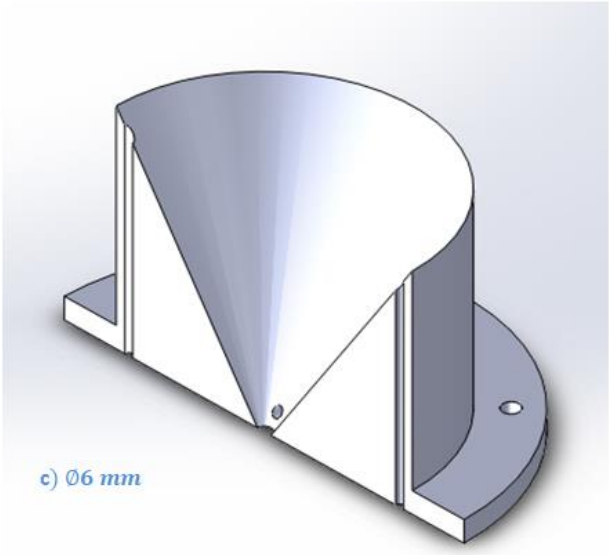

Figure 5.7 Cross-sections of the synthetic jet nozzles in the Solidworks environment, isometric axonometry. Respectively having an outlet cross section of a) $\emptyset 25mm$, b) $\emptyset 12mm$ and c) $\emptyset 6mm$. Courtesy of Agency for Science, Technology and Research (A*STAR).

During the design process, the bases of the nozzles were conceived with two symmetric holes, allowing for bolting them to the bottom of the cavity in which they are inserted, so that vibrations would not eventually allow for any clearance.

The upper part of the nozzles was built with an outer diameter exactly equal to the inner diameter of the cavity. At mounting, it was found that they could fit with a certain interference, dependent on the tolerances set on the 3D printer. It was also noticed that, in all the cases, this interference was enough to hold the nozzle inside the cavity with no perceptible fluid leakage at their interface.

Furthermore, small through holes were located in the base for the insertion of the temperature probes, to monitor the convection going on through the cavity. The first two ones pass through the base, conveying the probes roughly a couple of millimeters above the outlet section of the nozzle, inside the restraining cavity. The remaining pass through the nozzle extrude, parallel to its axis, to carry them up to a section very close to the diaphragm. The diameter for those was chosen to be the lowest possible (Ø2 mm) to reduce the flow wasted through them, subtracting in such a way cooling power to the jet. This solution allowed for an effective way to monitor the air temperature at both the inlet and outlet of the jet.

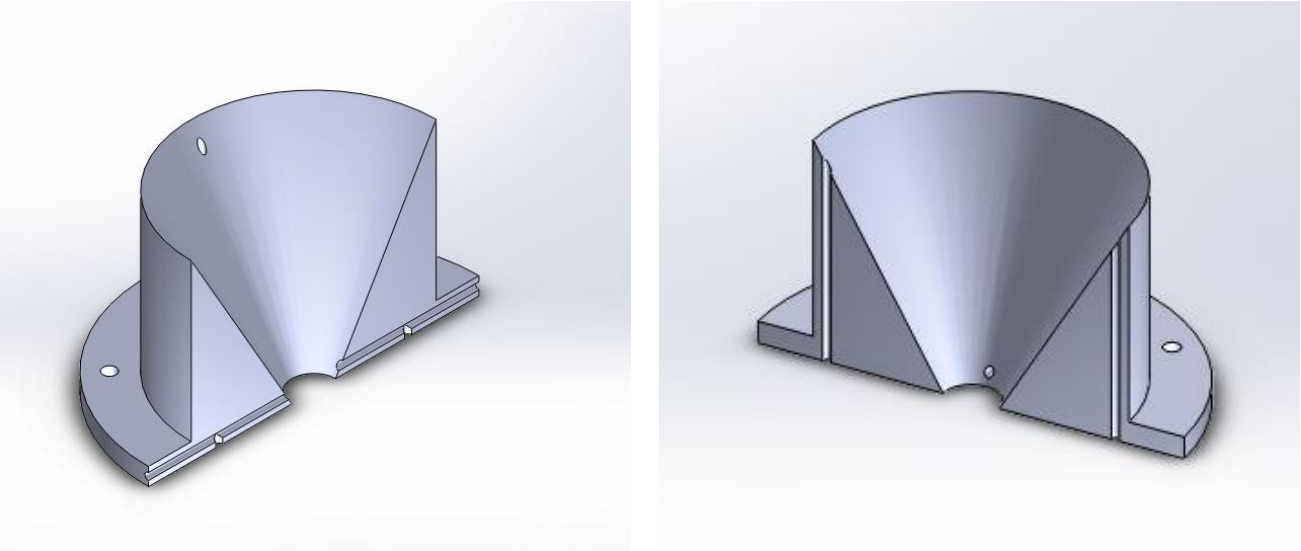

Figure 4.8 Mutually orthogonal cross-sections of the synthetic jet nozzles in the Solidworks environment, isometric axonometry. Courtesy of Agency for Science, Technology and Research (A*STAR).

4.3 DESIGNED COMPONENTS

The measurement of the loudspeaker displacement is fundamental for the sake of the whole analysis, as the parameters describing the flow inside the jet depend on it. Here is way the positioning of the sensor was treated with particular care.

4.3.1 Design of the support for the displacement sensor

The need for measuring with high accuracy the loudspeaker displacement introduced a new problematic: the positioning of the displacement sensor. Being its measuring range between 9 and 11 mm, a support was required to set it in place properly, so that it could be accordingly neared to the loudspeaker membrane.

In the preliminary design phase the requirements to satisfy could be summarized as follows:

- approximation of the sensor to the loudspeaker membrane, in accordance with the instrument measuring range;
- excessive vibrations avoidance;
- development of a readjust able support for the sensor;

The best way to meet the first two conditions implied that the support would hold the sensor without being mounted on the structure of the synthetic jet. It was rather found appropriate to bolt the support to the foundations of the synthetic jet.

Moreover, the measuring range is not the only variable determining the precision of the measurement. The CCD camera laser beam further add constraints to be satisfied. For it to be effective, the laser beam should be as much as possible

orthogonal to the surface whose oscillations are measured. It meant that the sensor needed to be properly oriented and readjusted through its support, depending on the setup arrangements. For the same support to be used throughout all the different tests it was necessary a readjust able one, with two degrees of freedom. The two were needed to satisfy respectively the condition of orthogonality and the one of the measuring range.

Being the two geometrical conditions differently oriented in the plane hosting the sensor head, it was conceived a support that could be moved in a polar reference system, rather than in a Cartesian one. So it was built with a slot and an hinge that allow for translation and rotation, respectively

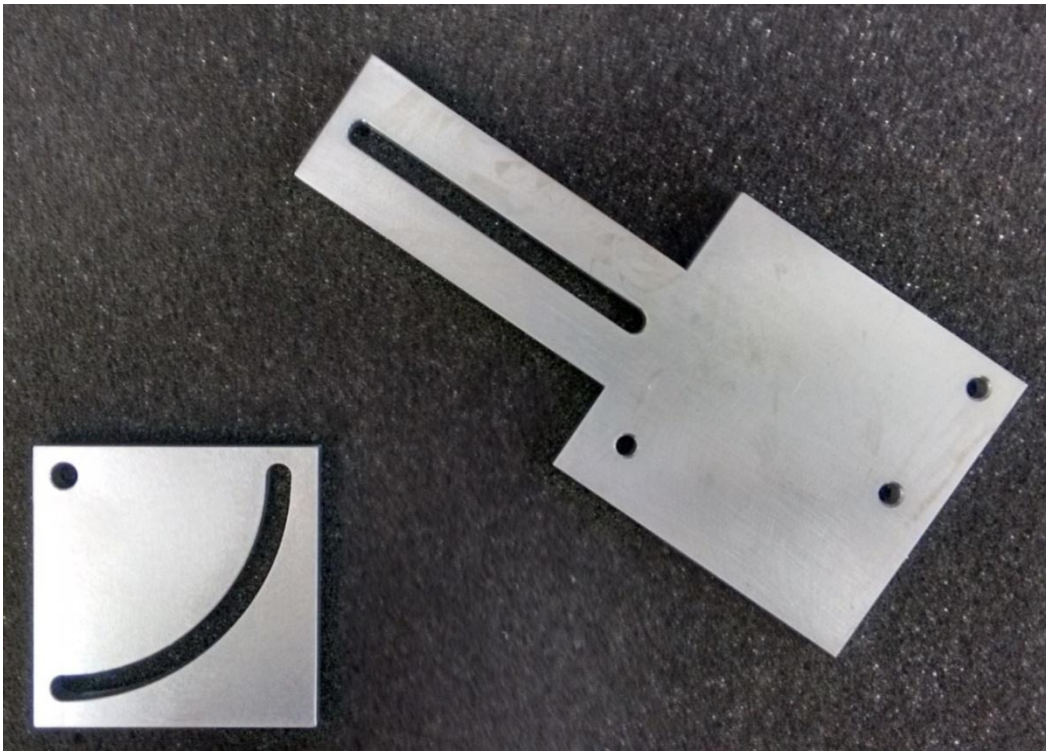

Figura 4.9 Two degree of freedom CMOS sensor support. Courtesy of Agency for Science, Technology and Research (A*STAR).

To first test the idea, a rough assembly of the synthetic jet was built in the Solidworks environment. Apparently, the support could satisfy all the requirements above mentioned, so it was sent to an external contractor for manufacturing. After only one week was ready, perfectly fitting in the setup. Even though the positioning of the support was found straightforward with the CAD simulation, the mounting tolerances and the space needed for the fixing bolts made the alignment slightly imperfect.

Unfortunately, the loudspeaker offered a black target surface for the laser beam, which did not allow for the best signal transmission. The problem was overcome by sticking a small piece of high adhesive metallic tape on the spot targeted by

the laser, big enough to always point it while oscillating, small enough to fit on the part of the surround that is stuck on the cone of the speaker. The tape adhesion was double checked before and after each test and no problematics were identified.

Figure 4.10 CCD camera laser beam target surface.Courtesy of Agency for Science, Technology and Research (A*STAR).

A greater amount of tape on the membrane would have slightly changed the membrane dynamics and affected the symmetry of the membrane. The adhesive properties of the tape, together with its own weight, added harmful tensions to the membrane functioning.

Furthermore, adding more tape did not showed to be successfully, practically. In fact, the complex geometry of both the membrane and the loudspeaker made so that the tape needed to be set in place with a few changes in geometry or, worst, by folding it at some points. The transmissibility of vibrations consequently increased and sometimes not even a complete test could be performed. However, no relevant drawback was observed, but the monitoring of the tape, in and between the measurements, was identified automatically as the safest practice to be included in the measurements protocol. It was also considered a good habit to substitute the tape once in a few tests.

4.3.2 A chassis to support the synthetic jet

The first prototype of the setup (see fig. 10)included a quite simple support for the synthetic jet, whose main functions were sustainment and prevention from changes of position due to vibrations. The need for a new copper plate required the design of a completely different chassis, since the first one was not big enough to allocate it under the jet.

Being time very precious for the experimental work, the design of another chassis was not dealing to the best scenario. Even though if designed on purpose, a single-piece chassis could have brought new, thus unknown, problematics once mounted; likely, those could have been solved just by the design of a new piece.

The bureaucratic, manufacturing and delivery times could have seriously compromised the execution of the tests, if more than a chassis was designed. Additionally, it was found interesting to introduce a second cylinder into the synthetic jet structure, identic to the first one, to test more mounting configurations. In particular, the first idea was to locate both of them in series. Thus, the new chassis needed to be higher than the first one with respect to the base of the setup.

Since the support was anyways needed, it was found worth to think broader. Modularity and readjustability were encouraged in conceiving the new one.

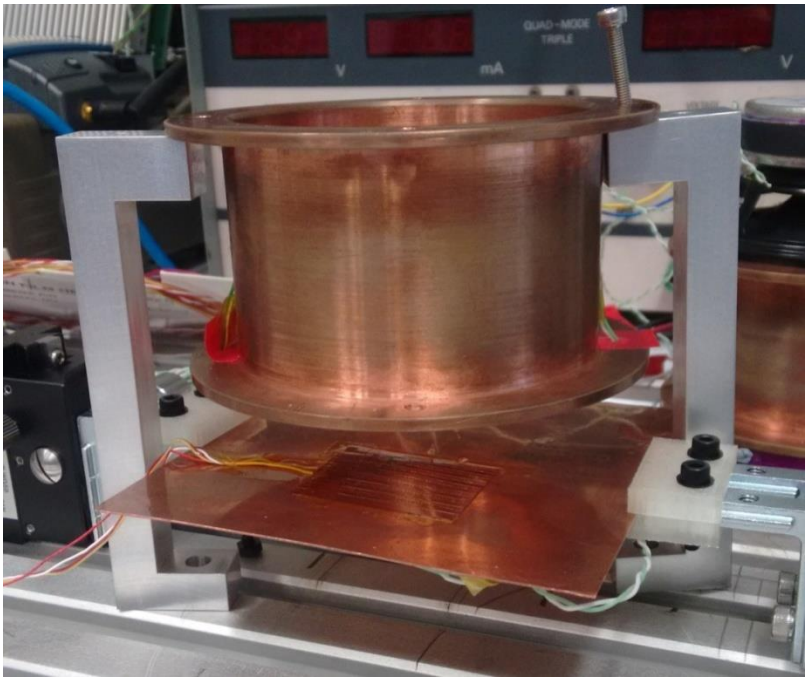

Figure 4.11 Mounting of the synthetic jet chassis. Courtesy of Agency for Science, Technology and Research (A*STAR).

Particularly, the new chassis consisted of four C-shaped thin beams, whose extremities were provided with a passing through hole (see fig.17). The one at the

bottom allowed for anchoring each beam to the foundation, while the second one allowed for the sustainment of the two cavities. The upper part of the cavity lies on the four C-shaped beams and could be fixed by bolting and used as single cavity synthetic jet. Nevertheless, this last part simply represented the basis of the chassis, as during all the tests whose data were collected two cavities were used to convey the flow on the plate.

4.3.3 Mounting a second cavity

Once the first cavity was mounted, it was guessed that the presence of a second cavity could better deliver the flow upon the plate. So it was proved to be. Particularly, the first cavity was left unchanged, while the second one was mounted on the top of the first one, hosting the nozzle. Such configuration proved to be more effective than the reversed one.

The flow intermittence was thus originated by the loudspeaker, went through a short entrance region in the second cavity, then restrained in the same one, then driven by the second cavity on the plate. In the mounting phase it was observed that leaving a clearance between the two cavities increased the performances of the device, allowing more fluid to be pushed and pulled back through the all air column, thus, on the target plate. An optimum clearance was set by hand and identified around 6 mm, parallel to the revolution axis of the cavities, orthogonal to the plate.

The setup explained in this paragraph was used throughout all the test whose data where collected, as this design configuration showed to be the most effective in cooling the plate in the phase of the preliminary tests.

4.4 THE FINAL SETUP FOR THE ANALYSIS

Once the synthetic jet chassis was found to perfectly fit in the setup, the whole was ready and functional for the tests and the relative data collection.

4.4.1 The foundation of the setup

The chassis of the synthetic jet was bolted to a heavy metal base, that will be hereby referred as the foundation of the system. Its weight secures the whole structure of the synthetic jet against vibrations. The base is a whole piece, machined so that a series of T-shaped slots were obtained, equally spaced. They are the main reason for using this specific base, as they allowed for effectively securing the synthetic jet chassis, the plate adjustment unit and the support for the displacement sensor. In tension against the T-slots for sustainment and securing

purposes, the nuts used to screw the fixing bolts were carefully surrounded by insulator tape, avoiding rigid metal-to-metal contact and the higher vibration transmissibility as a consequence.

4.4.2 Synthetic jet column

The synthetic jet chassis, as it has been carefully described in section 3.3.2, sustains both the cavities, together with the nozzle and the loudspeaker. Such assemble will be referred in this text as the “synthetic jet column”. The distance between the two cavities has been created by simply using three nuts as spacers, concentric with the through holes dedicated in both the cavities and in the nozzle. The loudspeaker has been simply bolted to the top part of the primary cavity, through the four dedicated holes.

The same holes at the bottom of the second cavity have been used “inappropriately” as rings to sustain the temperature probes that measured the temperature just above the target plate, placed at a distance from it that is approximately 1 mm. After different attempts, it was noticed that by making the probes passing through those holes and using a bit of adhesive tape was the best solution to resist the intermittence of the flow and the overall vibrations. In such a way it was guaranteed a certain repeatability for those measurements, as the probes were not find out of their place after each test. Although the stiffness of the cables of the temperature probes allowed a good positioning over the plate, it was good practice to double check their position before and after each test. It also was considered a conservative choice, considering the event of any external perturbation (i.e. vibrations from the equipment in the surrounding) affecting the foundation of the synthetic jet in the laboratory.

Two important elements surround the synthetic jet column: the plate adjustment unit and the support for the displacement sensor, respectively described in sections 3.1.2 and 4.3.1.

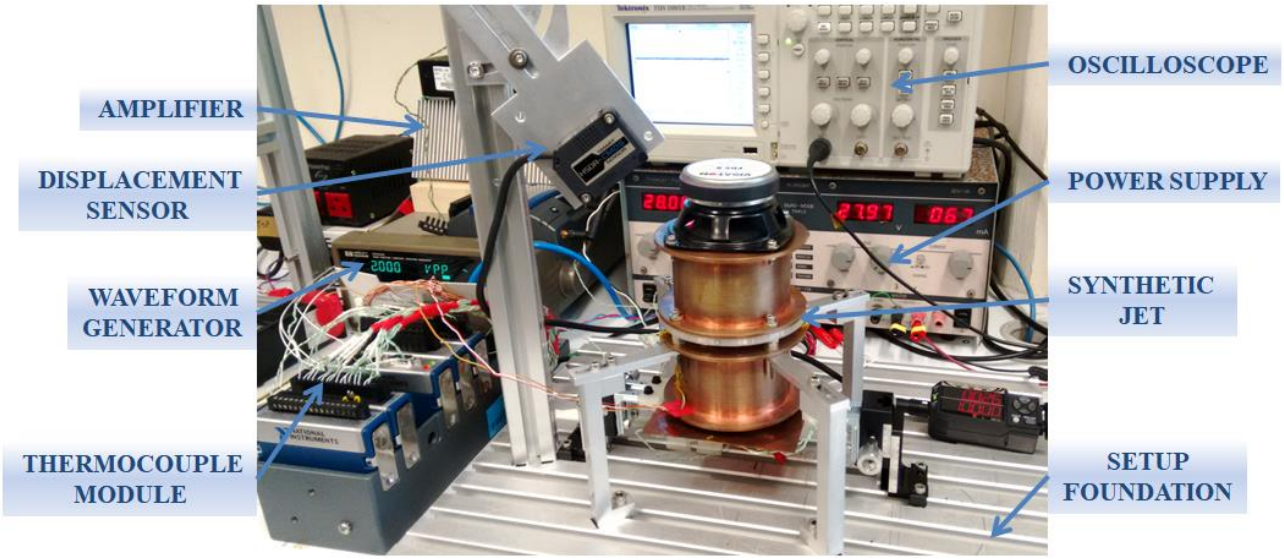

Figure 4.12 Full experimental setup. Courtesy of Agency for Science, Technology and Research (A*STAR).

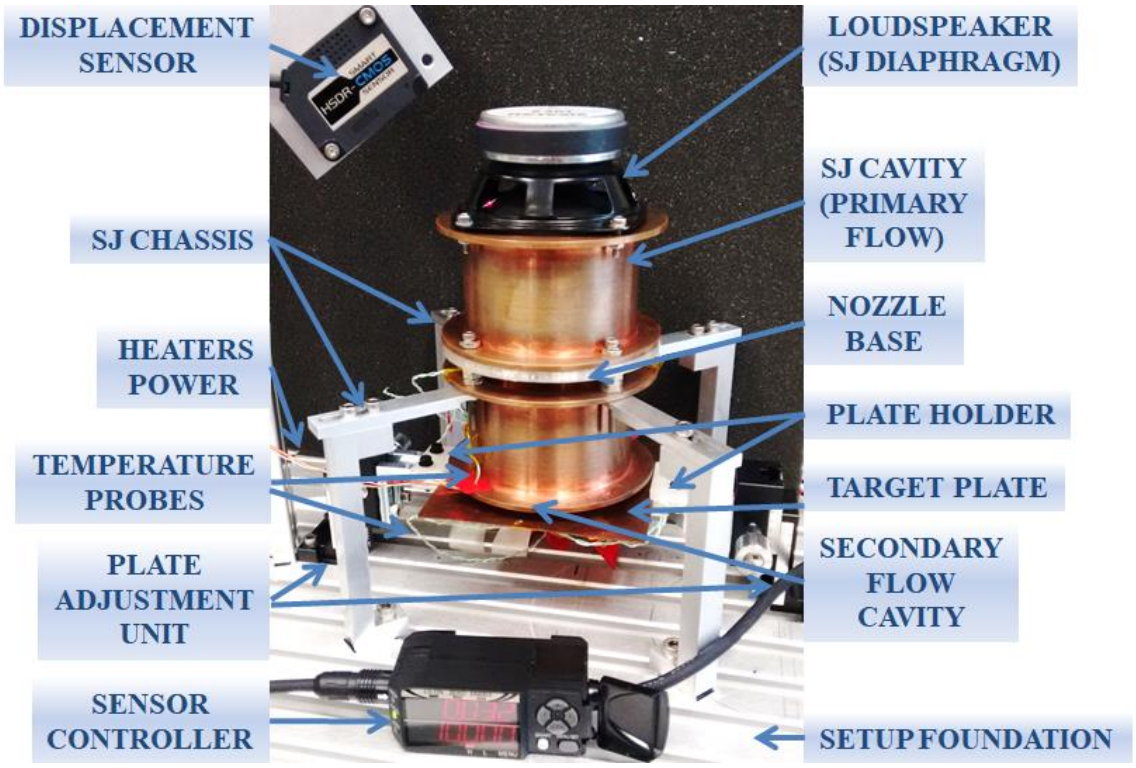

Figure 4.13 Zoom of the experimental setup on the sythetic jet system. Courtesy of Agency for Science, Technology and Research (A*STAR).

5| *EXPERIMENTAL TESTS*

The first weeks of the experience were fundamental for the design and development of the device, as well as for the definition of an experimental protocol to follow for data collection.

5.1 PRELIMINARY TESTS

Once the configuration described in the appropriate section was proved to be the most effective for the convection of the flow over the plate, a few tests were executed in order to determine the optimal clearance between the two cylinders conveying the flow.

5.1.1 Configuration of the cavities

Preliminary tests showed that the readjustment of the plate through the Misumi adjustment unit did not report sensible changes in the heat transfer enhancement over the plate but a simple increase in the plate temperature of 1-2°C (maximum) lowering the plate at the bottom of the unit. It makes sense as the values of the wavelengths investigated are sensibly higher with respect to the characteristic dimensions of the system and taking into account the range of values available, thus the slight difference in temperature could be attributed simply to a higher dispersion of the flow at the outlet of the second cavity. For this specific reason the plate was neared as much as possible to the outlet of the second cavity, being 8 mm the lowest clearance possible due to spatial constraints.

On the other hand, as figure 5.1 shows, the clearance between the two cavities showed to sensibly affect the overall boundary layer redevelopment, as it allowed the removal of heat flowing up through the jet column. The following distances were tested: 2, 3, 4, 5, 7, 11, 13, 15, 17 and 19 mm. The investigation of this height as a function of the operating point was neglected, as the purpose of the work was to develop a unique design optimal configuration and to evaluate the different results based on the operating point with that fixed configuration.

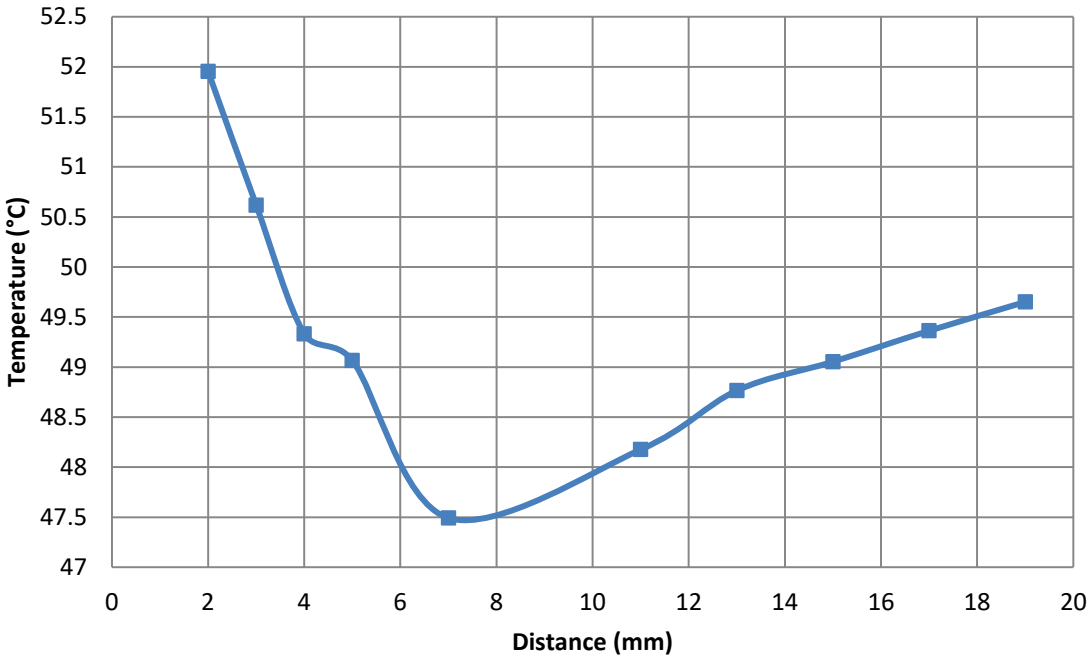

Figura 5.1 Mean value for the temperature of the plate as a function of the clearance between the two cavities.

Experimental evidence suggested the implementation of a 7 mm clearance.

5.1.2 Experimental conditions

The average pressure in Singapore during the experimental part of the work was 1010.28 mb. The static pressure P_0 has been set to 1000 mb mainly to comply with the dominant choice in literature. This value roughly accounts for the slight drop in pressure inside the laboratory, too. This semplification is reasonable, does not affect the analysis and makes so that it complies with experimental standards. The temperature of the free stream air in the laboratory was set to 26°C, as this value was the mean one recorded inside the laboratory at A*STAR.

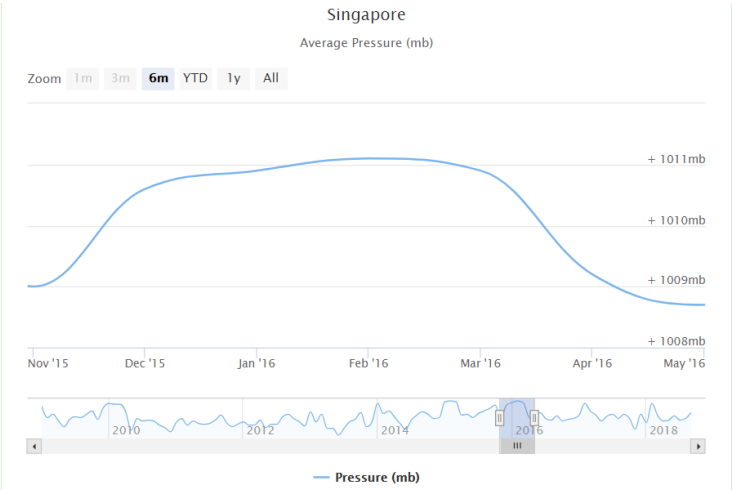

Figura 5.2 Plot of the average atmospheric conditions in Singapore during the experimental part of the work. Source https://www.worldweatheronline.com/ Accessed 04 April 2018.

5.1.3 Determination of air conductivity

To refine the non-dimensional analysis it has been appropriate to use up-to-date correlations for the calculation of air thermodynamics properties, hereby reported for the sake of completeness, with their respective ranges of validity [8]:

$$c_p = c_0 + c_1 T + c_2 T^2 + c_3 T^3 + c_4 T^4 \quad (5.1)$$

$$\mu = mu_0 + mu_1 T + mu_2 T^2 + mu_3 T^3 + mu_4 T^4 \quad (5.2)$$

$$k = ki_0 + ki_1 T + ki_2 T^2 + ki_3 T^3 + ki_4 T^4 + ki_5 T^5 \quad (5.3)$$

Tabella 5.9 Table of thermophysical properties of dry air according to [8].

Correlation coefficients	Temperature range	Units
$c_0 = 0.103409$ $c_1 = -0.284887x10^{-3}$ $c_2 = 0.7816818x10^{-6}$ $c_3 = -0.4970786x10^{-9}$ $c_4 = 0.107702410x10^{-12}$	[0 °C, 120 °C]	$\frac{kJ}{kgK}$
$mu_0 = -9.8601x10^{-1}$ $mu_1 = 9.080125x10^{-2}$ $mu_2 = -1.176355x10^{-4}$ $mu_3 = 1.2349703x10^{-7}$ $mu_4 = -5.797129x10^{-11}$	[-23 °C, 327 °C]	$\frac{Ns}{m^2}x10^{-6}$
$ki_0 = -2.276501x10^{-3}$ $ki_1 = 1.2598485x10^{-4}$ $ki_2 = -1.4815235x10^{-7}$ $ki_3 = 1.73550646x10^{-10}$ $ki_4 = 1.066657x10^{-13}$ $ki_5 = 2.47663035x10^{-17}$	[-23 °C, 777 °C]	$\frac{W}{mK}$

5.2 DATA ANALYSIS

As the typical factory tolerance for the resonance frequency of the speaker is ±15% (in our case, 18Hz, see table1), the gap between the testing frequencies has been conservatively chosen to be approximately twice this value. This assumption showed complete agreement with the results, as in the preliminary testing phase were chosen lower gaps (5, 10 and 20Hz).

Those last options would have been significantly time consuming for the sake of the whole analysis, so were archived as considered counterproductive. Particularly, it would have increased unnecessarily the time needed for testing. Furthermore, taking into account the amount of data available, it was considered more than enough in order to search for trends, patterns and relationships between all the variables involved in the analysis.

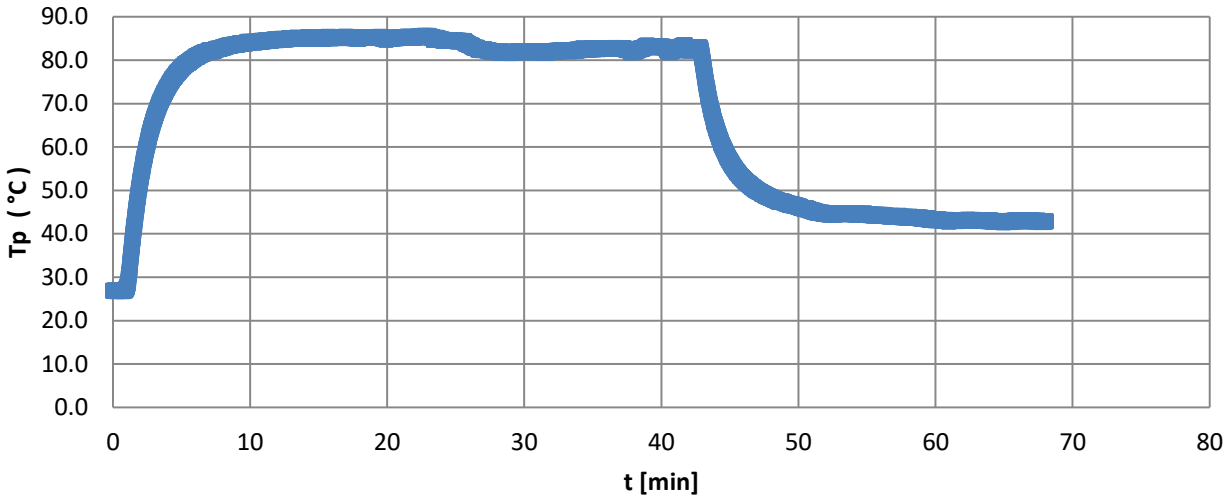

Figura 5.3 Sample of the temperature of the target plate with the synthetic jet working during preliminary tests at f = 100 Hz, V = 2V.

According to the protocol developed for testing, the operator should (in chronological order):

1) check temperature probes were properly connected, as vibrations or an eventual disassembly (i.e. for substituting the nozzle) could affect the adherence of the thermal tape;
2) turn on LABView interface and start recording data;
3) turn on the power generator, setting through the coarse control the voltage to 28 V with no current (0A) at first, set subsequently this latter to 0.370 A and refine carefully the value through the fine control for the sake of measurements repeatability – power on the plate is so around 10 W;
4) wait for the reach of a steady state temperature around 75°C, with the jet off, corresponding to the mean temperature recorded in the environmental conditions of the laboratory with natural convection, being 26 °C the ambient temperature;
5) set the amplitude modulation of the signal sent on the waveform generator through the AM signal button, set the voltage and frequency through the so labeled buttons, remembering to set enter the voltage in peak-to-peak V_{p-p};
6) turn on the power on the synthetic jet and wait for the transient to extinguish;
7) continue to record measurements of the temperature for at least a couple of minutes once the temperature over the plate is steady;
8) transfer data from the LABView text (.txt) to Excel for saving and subsequent import to Matlab for data analysis.

The final temperature recorded for data elaboration has been taken as the average of 25 values measured during phase 7), per each probe.

6|NON-DIMENSIONAL MODELING

6.1 DISCUSSION AND ASSUMPTIONS

Internal flows are frequently turbulent. In the case of synthetic jets, the turbulence plays the major role on the effectiveness of the cooling process.

Experiments [3] revealed that, if a fluid is subject to turbulent motion in a pipe, the details of the flow are likely to not be fully developed within 80 or more pipe diameters. Imagining to instantaneously visualize the velocity profile inside the synthetic jet cavity, it is possible to extrapolate a few considerations.

6.1.1 Cavity and nozzle: the model

The height of the synthetic jet is of the same order of magnitude of the average diameter of the synthetic jet column. This means that it is possible to model the flow throughout the whole cavity as if its profile is the same as in the entrance section, where the speaker is placed. This hypothesis is supported by the fact that the air viscosity is low; thus, the boundary layer thickness on both the cavity is negligible in the analysis. These assumptions allow for the calculation of the velocity at the exit of the synthetic jet by applying the continuity equation with respect to the entrance section.

Additionally, it is fundamental to notice that the loudspeaker effective piston area (31 cm^2) approximately equals the area of both the cylindrical cavities conveying the fluid on the plate (≈38 cm^2,without any nozzle). As the loudspeaker is in axis with the cavities, it is reasonable to consider the waves induced in the cavities as plane waves, especially considering that the air particles inside the chamber are subject to local frequent oscillation back and forth through it.

It deals to no significant error for the sake of this analysis to model the loudspeaker as a plane oscillating diaphragm at the entrance section of the synthetic jet. For all the above mentioned reasons, including the low viscosity of air, it is also reasonable to admit the flow is periodically perturbed by the propagation of plane acoustics waves inside the nozzles as well.

6.2 NON-DIMENSIONAL ANALYSIS

Non-dimensional analysis has been proven to be the most effective way to study most of the devices working with fluids. There are various reasons for it to be implemented and between the most relevant there are:

- formulation of criterions to evaluate the device performances;

- getting insights into the underlying physical phenomena, regardless of the system geometry and dimensional flow parameters;
- implementation of numerical methods;
- prototyping and modeling.

6.2.1 The synthetic jet criterion

Synthetic jets behavior has been successfully described through a simple "slug model", described in detail by (B. Smith A. G., 1998), (Glezer, 1998) and (B. Smith G. S., 2001) [5].

Utturkar et al. [4]. showed that the non–dimensional parameters governing the synthetic jet formation are the Reynolds and the Strouhal number.

6.2.2 Convection over the target plate

An investigation of the local heat transfer going on the impingement plate has been conducted as a function of two variables: the system design and its operating conditions. Both determine the dominant role of convection within the different heat transfer mechanisms.

The insulation system designed for the target plate makes so that a negligible fraction of the heat is conducted out of the plate. Additionally,the operating temperatures are sensibly lower than 100°C; thus, radiation was neglected in the whole analysis. For such a system the Nusselt number is the most relevant parameter in describing and estimating the heat transfer mechanisms, thus, the synthetic jet effectiveness.

6.3 JET PERFORMANCES

The first estimation of the jet performances focused on getting a practical knowledge of how the synthetic jet operating point determined changes on the convection over the heated plate.

The operating points were set through the waveform generator:

1) frequencies of the loudspeaker: 60, 100, 120, 140 and 180 Hz
2) voltage of the loudspeaker: 2, 3, 4, 5, 6 V

All the voltage values have been tested per each frequency, and so was done per each nozzle, resulting in a final number of 75 tests. Many additional preliminary tests were also performed in the preliminary part of the experimental work, and various have been saved with their respective protocols, reporting different

measurements and testing conditions. For the sake of synthesis will not be reported, as they were meant to:

1) gather information to support the design and the development of the system;
2) elaborate a complete robust protocol that conservatively expected to take more measurements than those apparently needed during the experimental part of the work. This guess turned to be fundamental at a later stage, as the elaboration of data was continuously updated and refined with the aims to be comparable with other research works and to get new insights.

As those files allow to extrapolate information about the behavior of the jet as a function of other variables than those investigated in the analysis (i.e. the height of the jet column or the behavior at higher frequencies), those interested in the topic could address anytime the author of this thesis at engpiernich@gmail.com.

Referring to figure, the diameters a), b) and c) will be respectively called D1, D2 and D3, for simplicity.
Thus, recalling these values:

1) D1 = 25 mm;
2) D2 = 12,5 mm;
3) D3 = 6 mm.

The distance between the outlet section of the nozzle and the target plate has been set to a fixed value, corresponding to 80 mm: being 8 mm the clearance between the target plate and the outlet of the cavity carrying the secondary flow, 63 mm the height of this latter, whose inlet is 10 mm the distant from the outlet of the synthetic jet.

It is appropriate to introduce the aspect ratio, that is the ratio between the distance of the outlet of the synthetic jet and the target plate, which allows to extend the results to other research work by non-dimensionalizing the diameter of the jet as follows:

$$AR = \frac{H}{d} \tag{6.1}$$

Where H is the distance of the outlet of the synthetic jet section from the target plate, measured in the direction in which convection occurs.

Table 6.6 Summary relative to the range of values set on the waveform generator throughout all the saved tests.

Operating point variable	Range
V	2, 3, 4, 5, 6 V
f	60, 100, 120, 140, 160, 180 Hz

Table 6.2 Summary relative to the range of aspect ratioss throughout all the saved tests.

Nozzles	Diameter	AR
D1	25 mm	3,2
D2	12,5 mm	6,4
D3	6 mm	13,3

6.3.1 Effect of the operating point

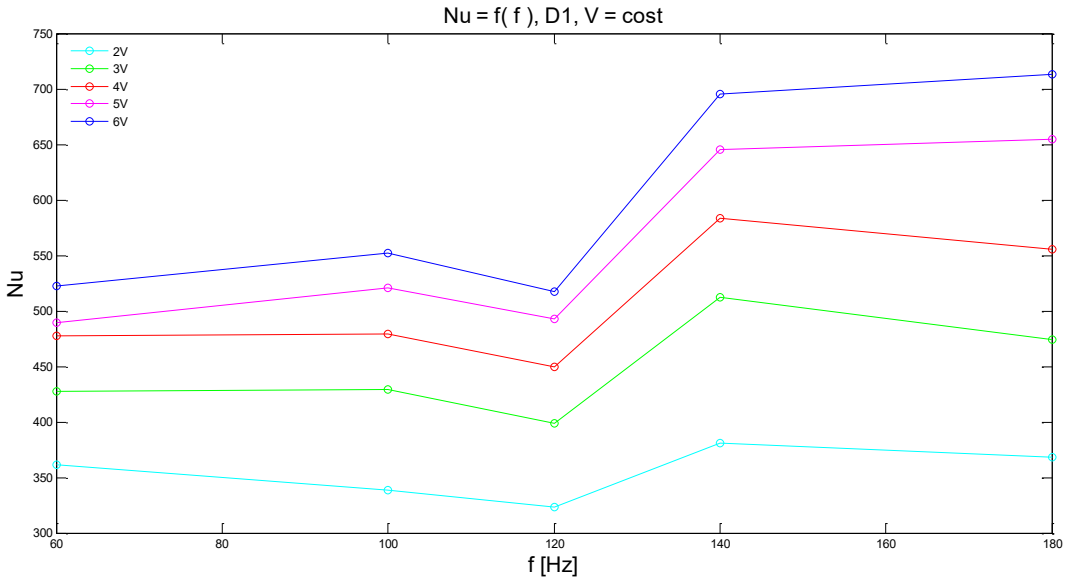

Figure 6.1 Nu number as a function of the operating frequency, one per operating voltage. D1 = 25 mm.

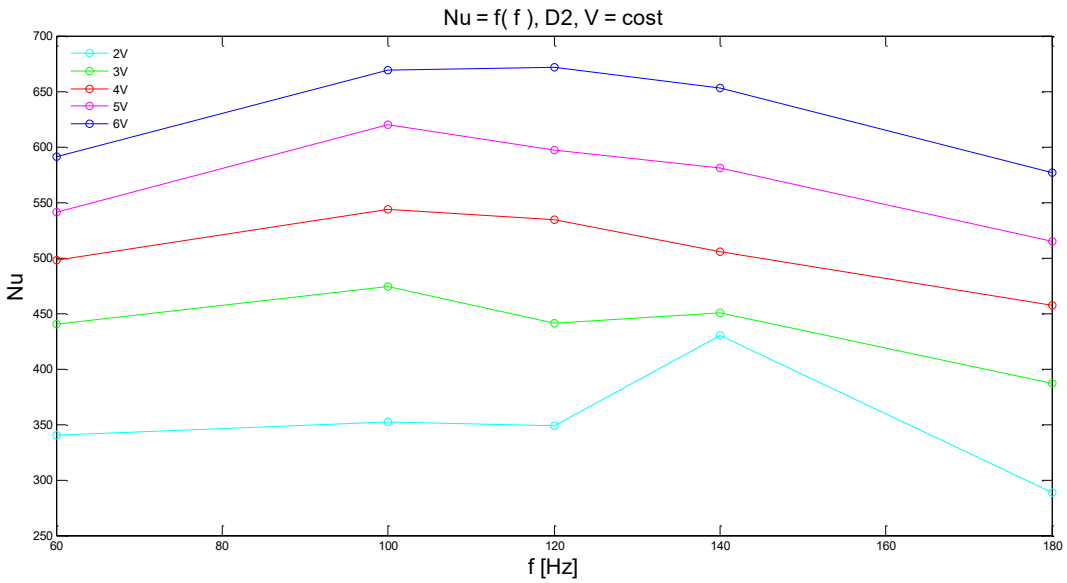

Figure 6.2 Nu number as a function of the operating frequency, one per operating voltage. D1 = 12.5 mm.

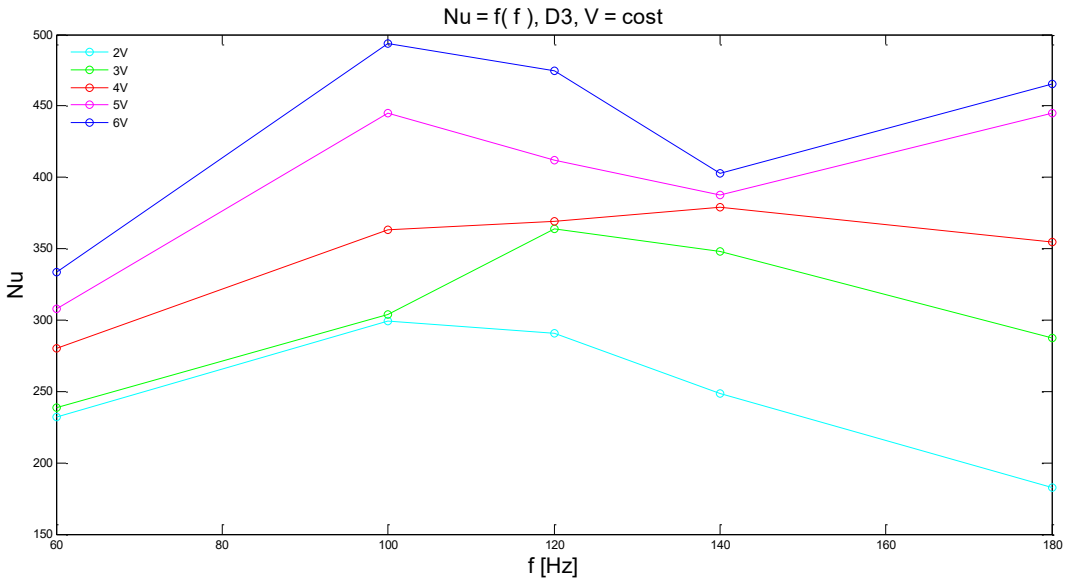

Figura 6.3 Nu number as a function of the operating frequency, one per operating voltage. D1 = 6 mm.

The bidimensional graphs above listed were useful to extrapolate the first insights about the change in behavior of the synthetic jet depending on the frequency, that has been identified as the dominant variable to determine the output on the target plate temperature.

Throughout the graphs emerges that the Nusselt number increases monotonically for all the jets with the increase of the voltage set on the waveform generator.

The coil velocity of the speaker is directly proportional to such voltage; thus, the resulting higher rms velocities within the cavity determine an enhancement of the mean flow over the plate throughout all the frequencies.

The absolute maximum of the Nusselt number over all the performed tests reported an heat transfer enhancement higher than 7 times the one corresponding to natural convection. This maximum occurs at the upper boundary of the set of data available, with respect to both the voltage and the frequency; but the map of the tests and the speaker data sheet confirm the idea that a further increase of those values could have likely determined an higher Nusselt number. Particularly, nozzle D3 showed the highest performances, but its drawback is that the range of operating parameters determining high performances reduces significantly with respect to D2. The peak of those performances is partially due to the significant reduction in the cavity diameter, determining higher acceleration rates of the mean flow through the nozzle because of its reduction in area, but mainly by the speakers dynamics.

The nominal impedance of the speaker is 4 Ω, but in reality there is a variation of such value that cannot be neglected around the resonance frequency, so that the effect of mass transfer due to the resonance frequency is smoothed by the higher electrical impedance; as it would correspond to a decrease in voltage, which is know to determine a decrease or a drop of the Nusselt number.

The peak of the performances shifts its by changing nozzle due to various reasons:

1) the increase of the compression ratio of the nozzle accelerates the flow;
2) the reduction in area acts as a resistance to the information of the backpressure travelling down from the diaphragm to the target plate. The fluid dynamic losses through the smaller nozzle for sure play a role in reducing its performances, but it is more important to recall that in this case a reduction of the nozzle also corresponds to an effective reduction of the heat transfer area over the plate.

The effect of the diameter reduction is analogous to hypothetical substitution of the loudspeaker with a smaller one, which would mean, in the hypothesis of a fixed value of SPL, a need for higher frequencies to compensate the reduction in flow redevelopment over the plate. Thus, the peak of the performances for the nozzles in usage shifts gradually from 60 Hz (D1), to 120 and 180 HZ for D2 and D3, respectively. Furthermore, it should be noticed that the peak of the performances at 6V and 180 Hz is mainly due to concomitant effects of the SPL increase and the speakers impedance decrease, as looking at the graph in figure the gap between the two curves is the highest throughout all the set of data. effects of the SPL increasing (Additionally, at low frequencies (i.e. 60 Hz in this

case) the speaker diaphragm is still quite stiff, thus the velocity of the diaphragm is generally overestimated)

The latter on the contrary has proved to be the most suitable nozzle for the system under analysis, as it provides high versatility of usage with a smoother drop of the performances around the speaker resonance frequencies, that is where the peak of the Nusselt number has been registered, too.

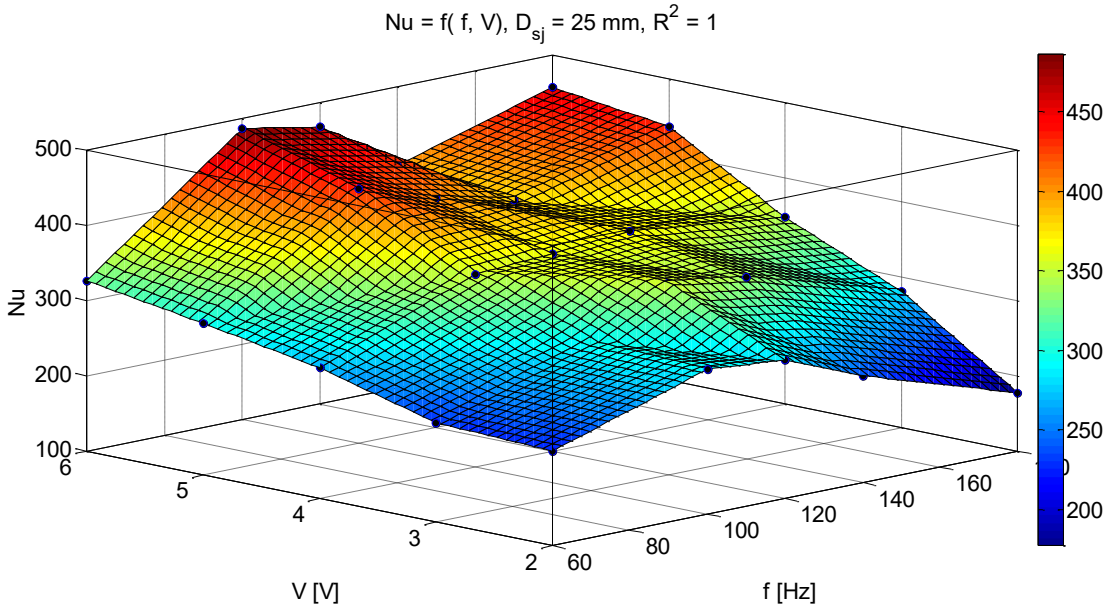

Figure 6.4 3D interpolation of the Nusselt number as function of the operating parameters, function for D = 25 mm.

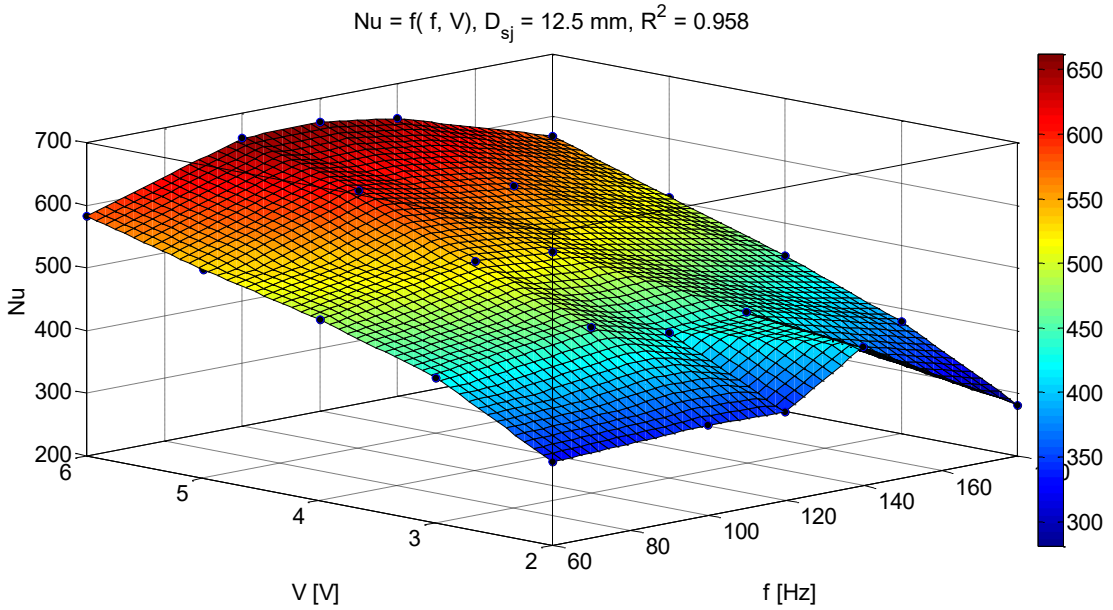

Figure 6.5 3D interpolation of the Nusselt number as function of the operating parameters, function for D = 12.5 mm.

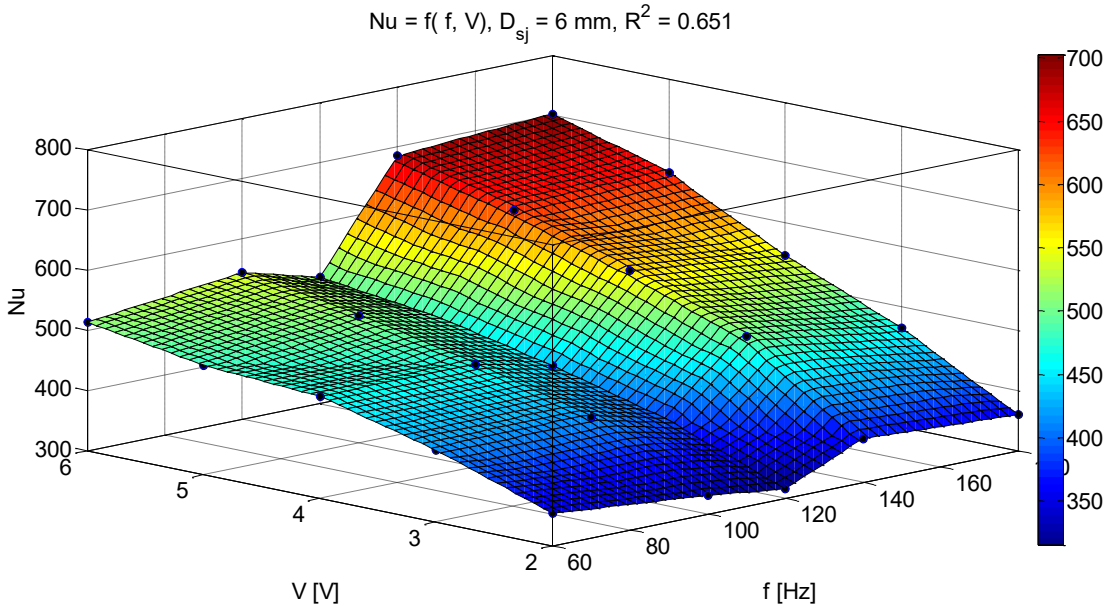

Figure 6.6 3D interpolation of the Nusselt number as function of the operating parameters, function for D = 6 mm.

The above listed graphs have been obtained in the Matlab® environment, using the 'scatteredInterpolant' data function, particularly suitable for interpolation of experimental data. It emerges clearly that an increase of the aspect ratio enhances convection over the target plate at first, because the effect of accelerating the flow through a smaller nozzle prevails over the reduction of the impinging outlet area. Thus, decreasing by half the first diameter it results an average increase in the Nusselt number of 143%. The reduction in diameter turns to be a positive effect in enhancing the convection only up to halving the first diameter, D1, as the smallest of the nozzles (D3) reported already a decrease of the Nusselt number by 3% with respect to D2.

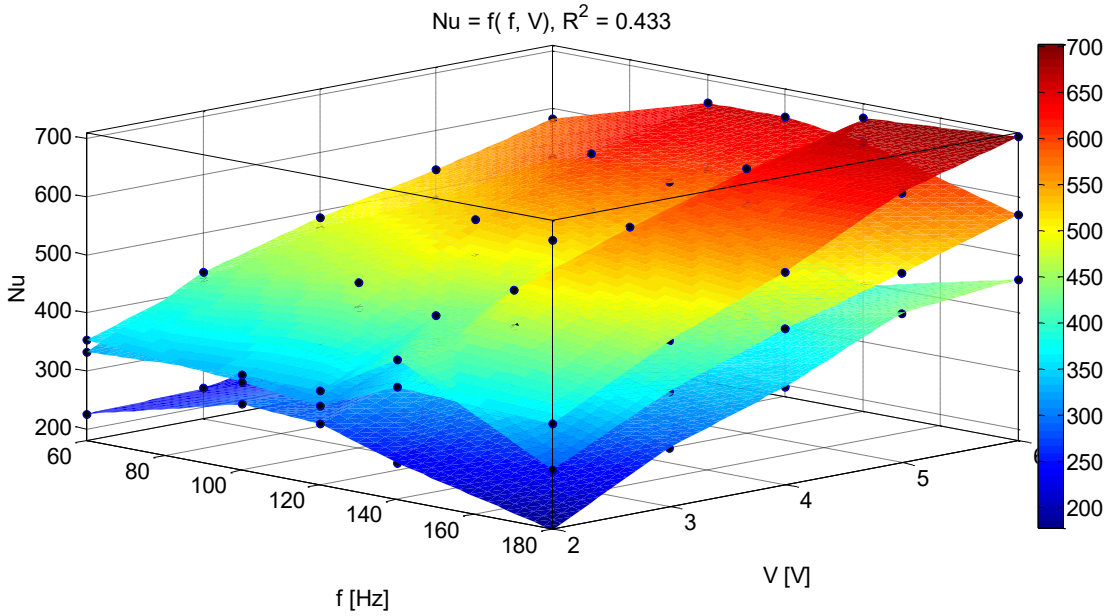

Figura 6.7 Comparison between the interpolant functions plotted in fig 6.4, 6.5 and 6.6 respectively, front view.

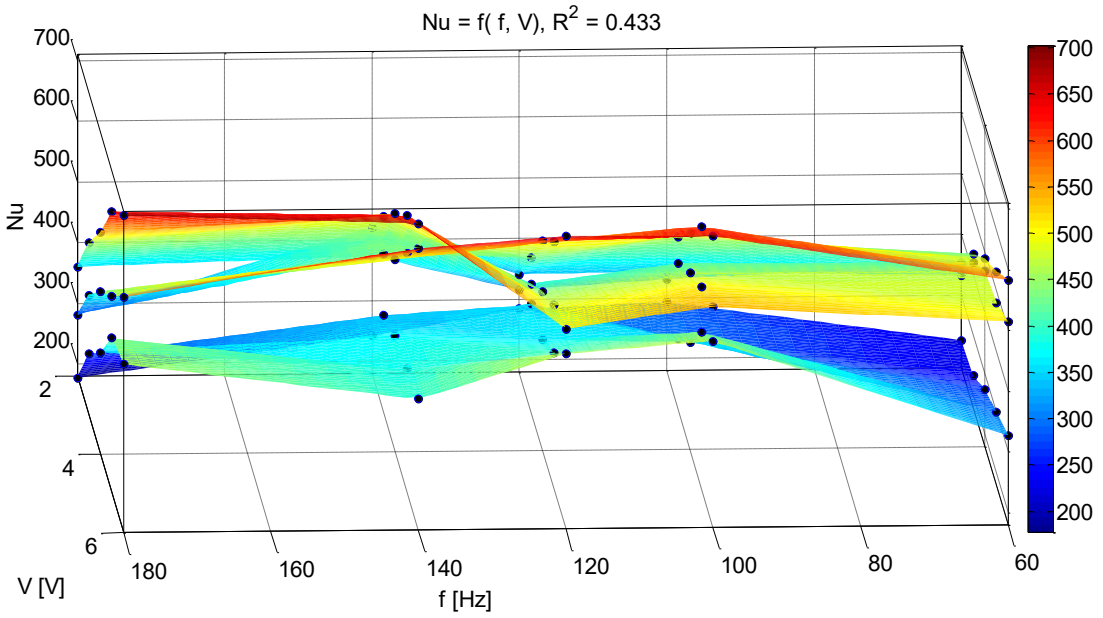

Figure 6.8 Comparison between the interpolant functions plotted in fig 6.4, 6.5 and 6.6 respectively, back view.

7| *MODELING THE SYNTHETIC JET*

Both the presence of non-linearities and multiple sources of losses determine a common tendency in the fluid machinery domain: the representation of the performances of the device through maps, rather than analytical expressions. One of the main aim of the experience, that was set during the experimental part of the work, was the tracing of a non-dimensional map that could identify the operating point and the efficiency of the synthetic jet. The number of variables determining the synthetic jet efficiency brought the need for a quick way to read its performances, in the perspective of industrial applications of such device.

Nevertheless, the evaluation of the conditions on the target plate based on the flow determined by the synthetic jet requires the analysis of the perturbation induced from the loudspeaker into the chamber and, consequently, over the plate.

The d'Alembert equation revolutionized the field of acoustics as allowed for a deterministic description of the motion of the air particles driven by a sound source. Particularly, it is important to state a few important outcomes of the gas dynamics. At any point invested by sound waves:

1) pressure and particle velocity are in phase, while the particle displacement is 90° out of phase with respect to the pressure changes;
2) the speed of sound is finite. Thus, the flow oscillates locally with the same frequency of the sound source, but not synchronously, so that an integral number of wavelengths separate two particles in exact phase along a wave;
3) the air perturbation travels in the same direction of the wave, as they are longitudinal.

7.1 COMPARING TWO MODELS FOR THE DETERMINATION OF NON-DIMENSIONAL PARAMETERS

This session will briefly describe the results of the first part of the elaboration of data, stating the reasons that suggested the implementation of an acoustic modeling of the system.

7.1.1 Fluid dynamic parameters based on a mechanical model

Particularly for synthetic jets, it has been found possible to describe the flow through different non-dimensional parameters. Noticing that the velocity of the pulsating flows a crucial variable in determining the synthetic jet effectiveness, it

is relevant for the sake of the whole analysis to introduce the Reynolds number, defined as:

$$Re = \frac{U_0 d_{sj}}{\nu} \tag{7.1}$$

where:

d_{sj}: diameter of the synthetic jet at the exit of the nozzle;

ν: kinematic viscosity of the air;

$$U_0 = f \int_0^{\frac{T}{2}} u_0(t)\, dt \tag{7.2}$$

with:

$u_0(t)$: spatial-averaged velocity at the d_{sj} section;
f: operating frequency of the synthetic jet.

Being difficult to implement this definition with the equipment in the setup, it was rather found that the assumptions stated could simplify the analysis.

Since each test was performed by running the loudspeaker at constant amplitude and frequency, it is possible to study the motion of the diaphragm as a sinewave defined by those two parameters. For the sake of the analysis:

- the value of the frequency was set and read on the waveform generator;
- the value of the amplitude was set on the waveform generator, but read on the oscilloscope connected to the displacement sensor.

The high accuracy of the displacement sensor allowed for the effective measurement of the diaphragm oscillations amplitude, avoiding the calculations on the loudspeaker motion of the piston. Between all the readings available, it was chosen the peak-to-peak value, as it was the most repeatable. Rather, to give an estimate of the intermittent flow going through the jet during a cycle, it was found more reasonable to convert this value into the root-mean-square value. It is possible finally to fully define the Reynolds number according to eq. 1, by rewriting the variable U_0 in terms that apply to this analysis as:

$$U_0 = \frac{f X_d}{\sqrt{2}} \tag{7.3}$$

with X_d being the total distance travelled by the diaphragm over one cycle of oscillation.

Being the flow inside the cavity intermittent, the Reynolds number does not provide enough information to characterize it. While an estimation of the changes in momentum inside the cavity periodically brought by the diaphragm

oscillations. It means that a second parameter needs to be introduced in the analysis, as a complement to the Reynolds number: the Strouhal number.

Evidences (Utturkar, 2003) were found about the crucial role of the flow intermittence on the efficiency of synthetic jet. If Strouhal numbers are sensibly high, the exchanges in momentum can become so intense that no clear jet is released from the orifice of the cavity. What can rather be observed is a local intense perturbation of the flow, on a micro scale. It also means that devices designed for meso-scale applications cannot work efficiently in the conditions estimated by the Strouhal number itself.

7.1.2 Mechanical approach

The implementation of a mechanical model based on the measured variables related to the motion of the loudspeaker was the first one to be suggested by intuition with the available equipment. In practice, definitions and calculations as defined in paragraph 4.2.1 were implemented.

The graphs that were obtained with such a model of the system were not satisfying to be considered the outcome of the analysis due to a series of reasons:

1) the motion of the air adhering to the loudspeaker (no slip condition) is not transferred rigidly over the target plate;
2) the speed at which the variation in pressure travels within the flow is the speed of sound; being the latter a limited one it results a delay in the arrival of the signal over the target plate;
3) the calculation of the diaphragm rms speed cannot take into account the aerodynamic losses within the cavity;
4) there might have been sources of errors in the determination of the diaphragm displacement, see paragraph 3.3.1;
5) the number of non-dimensional parameters that could be computed with the available equipment was not enough to get significant insights regarding the performances of the device;
6) the graphs resulting from the analysis were not well connected surfaces, with peaks and valleys whose identification and characterization would have complicated unnecessarily the interpretation of the results.

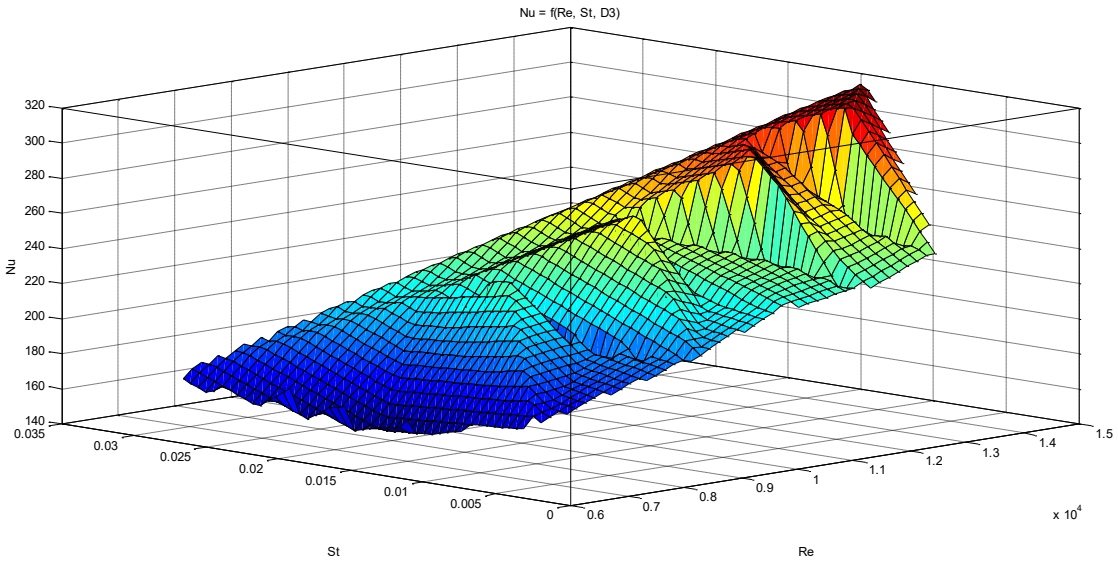

Figura 7.7 Three dimensional plot for the Nu number as a function of the operating parameters using the mechanical approach. Nu = f(Re, St) with AR = 13.3.

.7.1.3 Hypothesis about the loudspeaker

The modeling of the synthetic jet cavity and the simplifying hypothesis allowing for the calculations reported in this work will be hereby discussed and argued, with regard to the driver; that is, the loudspeaker.

In the case of a flat piston (or diaphragm):

1) vibrating at a fixed frequency;
2) placed at the end of a cylindrical tube;
3) having a small characteristic length with respect to one-sixth of the wavelength at which it oscillates;

It is possible to:

1) consider the loudspeaker as a point source radiating sound in the surroundings;
2) model the sound wave as a plane progressive wave travelling through the cylinder.

7.1.4 Reynolds and Strouhal number determination

Those two parameters are fundamental in order to identify the mean flow reaching the target plate and its degree of intermittency.
The velocity that accounts for the mean flow reaching the plate is given by the root mean square over the time of the wave velocity at the plate surface. This value has been computed following an energetic approach, which was identified

to be the most suitable with the available data about the speaker. Being the behavior of the speaker non-linear over the domain of the frequency, the most accurate way to determine the mean perturbation of the velocity of air was provided by reading the Sound Pressure Level diagram provided by Visaton®.

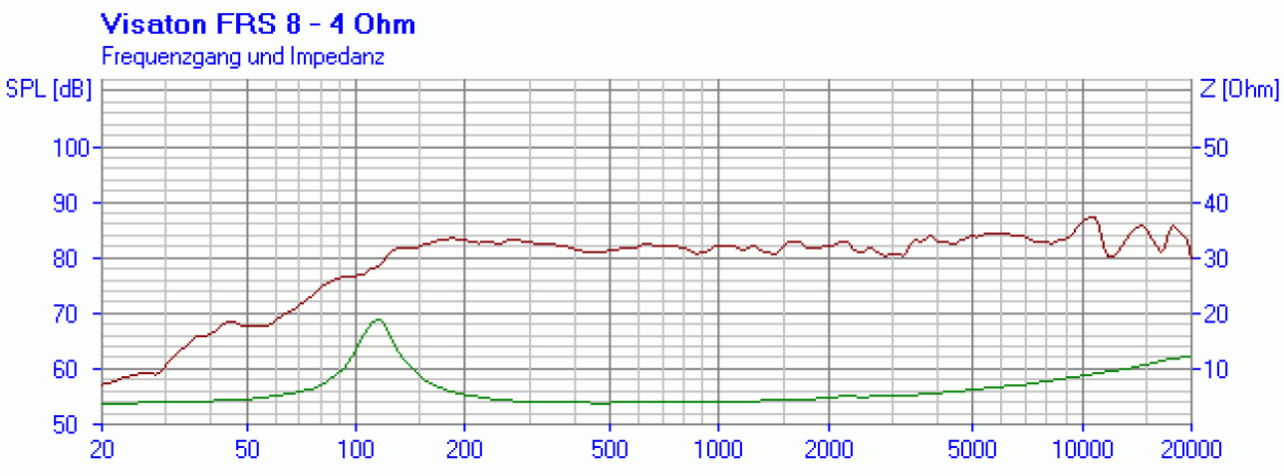

Figure 7.8 Visaton FRS 8 Art. No. 2003 impedance and SPL curves. Source http://www.visaton.de/en/products/fullrange-systems/frs-8-4-ohm. Accessed 13 Apr 2018.

By entering this graph with the operating frequency of the loudspeaker it is possible to determine the SPL in dB that is emitted by the loudspeaker given one watt of acoustic power, measured at one meter of distance from the loudspeaker. From (paragraph 2.2.1) it turns out that the determination of the mean pressure perturbation caused by the sound wave through equation(equation) allows also for the calculation of the sound intensity at that particular point, distant one meter, through:

$$I_{1W/1m} = \left(\frac{p^2}{\rho_0 c}\right) \tag{7.4}$$

It is possible now to determine the pressure perturbation over the plate, not before formulating the hypothesis that allow for such calculation:

1) the range of frequencies and the range of operating temperatures do not determine sensible differences in terms of sound absorption, being the distance of the plate of the order of 10 cm and the decay of sound in the average experimental conditions is less than 0.10 dB/m;
2) the percentage of acoustic power absorbed by the equipment and dispersed in the surroundings is supposed to be constant throughout all the tests, as the range of operating frequencies is particularly restricted to a narrow gap around the resonance frequency of the speaker. This assumption does not affect the information of the mean flow reaching the plate and its re-

development, as those depend basically on the operating conditions of the loudspeaker;

At this point it is possible to estimate the sound intensity reaching the nozzle, by taking into account its drop with the square of the distance and multiplying this value by the power supplied to the loudspeaker W_{ls}, it results:

$$I_{sj} = \frac{W_{ls}}{1W}\left(\frac{1m}{r_{sj}}\right)^2 \cdot I_{1W/1m} \tag{7.5}$$

where r_{sj} is the distance of the plate from the loudspeaker, measured vertically.

Determining the entity of the pressure perturbation at the synthetic jet through equation:

$$p_{sj} = \sqrt{\rho_{sj} c_{sj} I_{sj}} \tag{7.6}$$

It is at this point possible to enter the variables hereby defined, together with those in paragraph 2.2.1, and perform the non-dimensional analysis according to definitions given in their respective paragraphs.

8| *RESULTS*

This session will provide experimental results, graphs and data interpretation. Particularly, in accordance with the title of this thesis, there will be a focus on the two main variables determining the synthetic jet performances: the design and the operating point.

8.1 NON-DIMENSIONAL MAPPING

The following session will report all the observations coming from the elaboration of the non-dimensional analysis. Three dimensional mapping has been chosen as the main vehicle for those, as it helps the visualization of the phenomena hereby discussed.

8.1.1 Dependence of the Eu number on the Re and St numbers

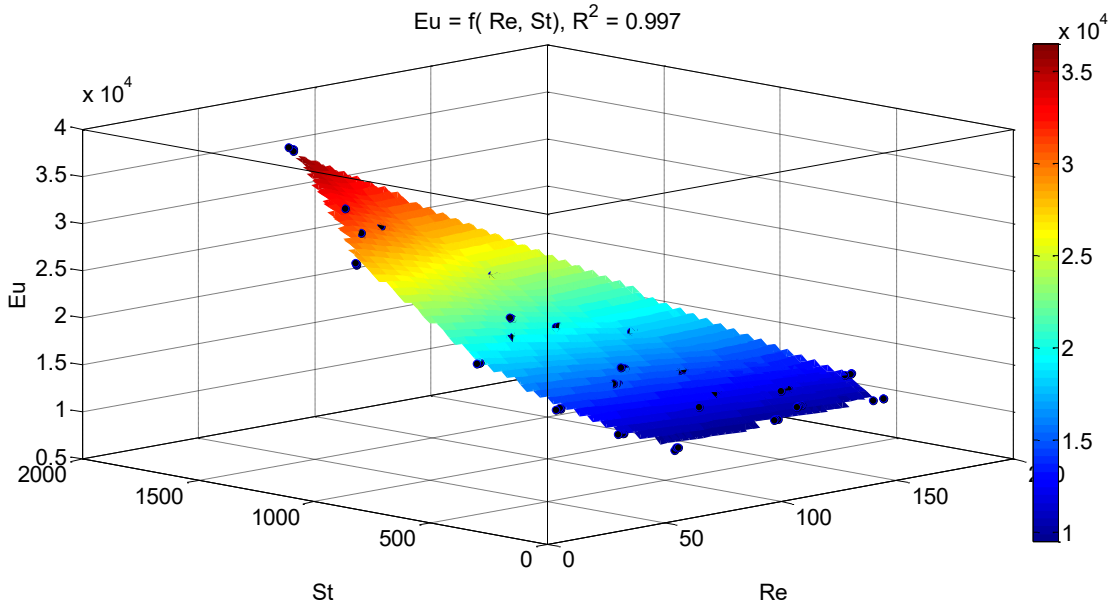

Figura 8.1 Three dimensional plot of the of the relationship Nu = f (Re, St) for all the tested AR.

Particularly for the case of the three non dimensional parameters related to the fluid dynamics of the system, it has been straightforward the identification of a polynomial interpolant function of the second order per each of the independent variables - valid for all the nozzles tested - whose linear fit with the experimental data reported a 0.997 coefficient of determination.

$$Eu = -3382 + 40.13Re + 34.65St - 0.02998Re^2 - 0.08899ReSt - 0.004159St^2 \quad (7.7)$$

8.1.2 Effects of the Re/St ratio and of Eu number on the performances

Previous studies focusing on the efficiency of synthetic jets enlighted about the importance of the Reynolds to Strouhal numbers ratio [4]. The importance of those parameters in fluid mechanics literature is very well recognized, while the crucial role of this variable in the present analysis can be sensed recalling the information that those numbers provide about the flow. As they are respectively a quantitative estimation of the mean freestream flow over the target plate and its degree of intermittency.

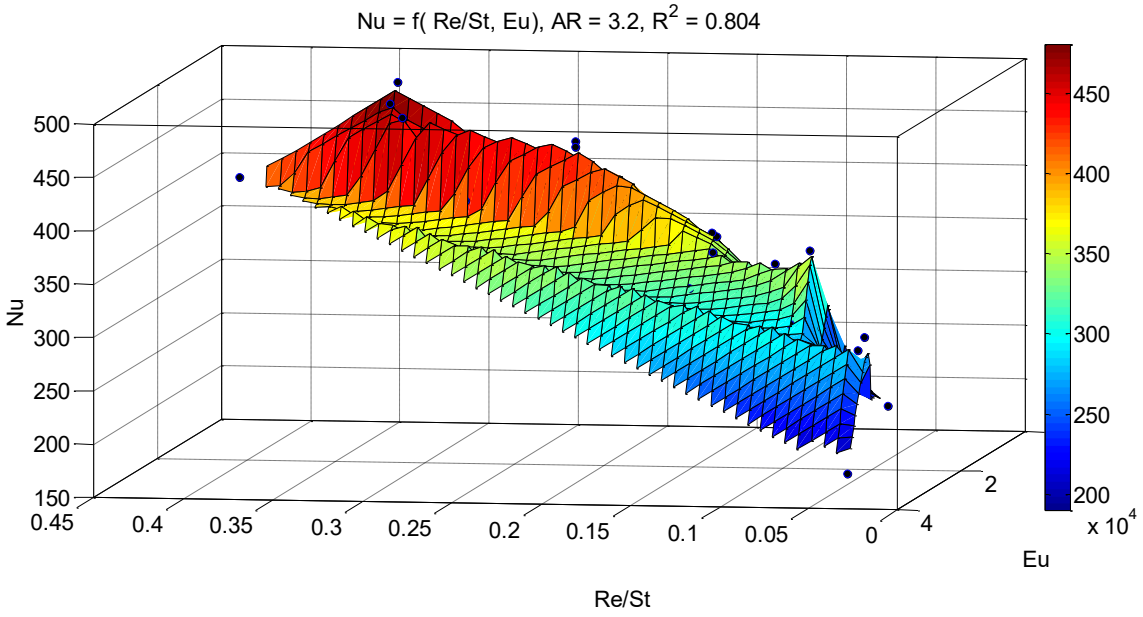

Figure 8.2 Three dimensional plot of the of the interpolating function for the relationship Nu = f (Re/St, Eu), AR = 3.2.

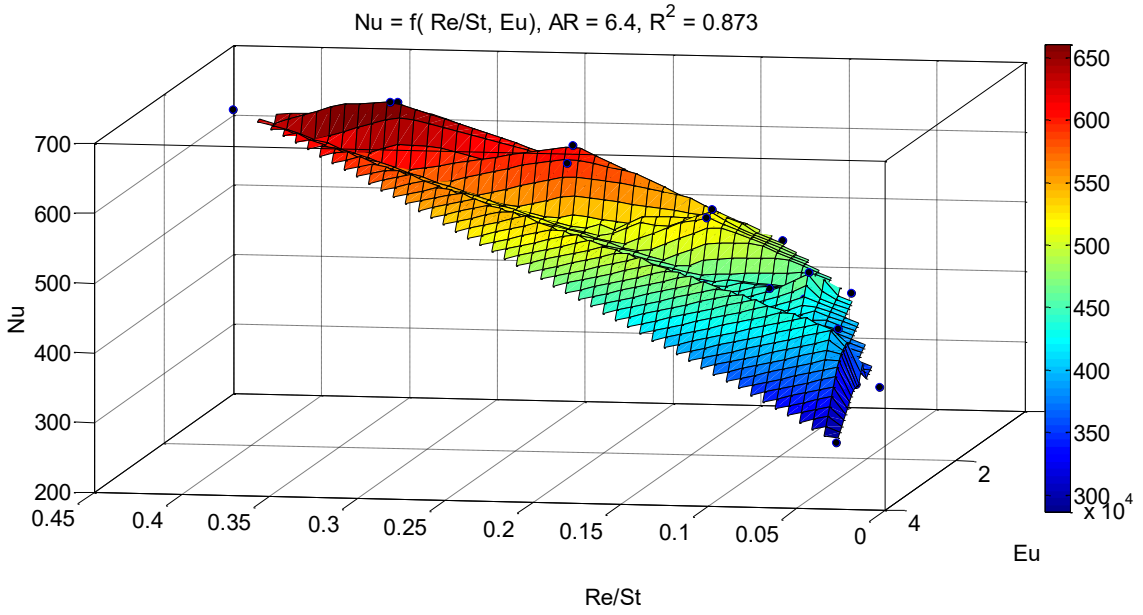

Figure 8.9 Three dimensional plot of the of the interpolating function for the relationship Nu = f (Re/St, Eu), AR = 6.4.

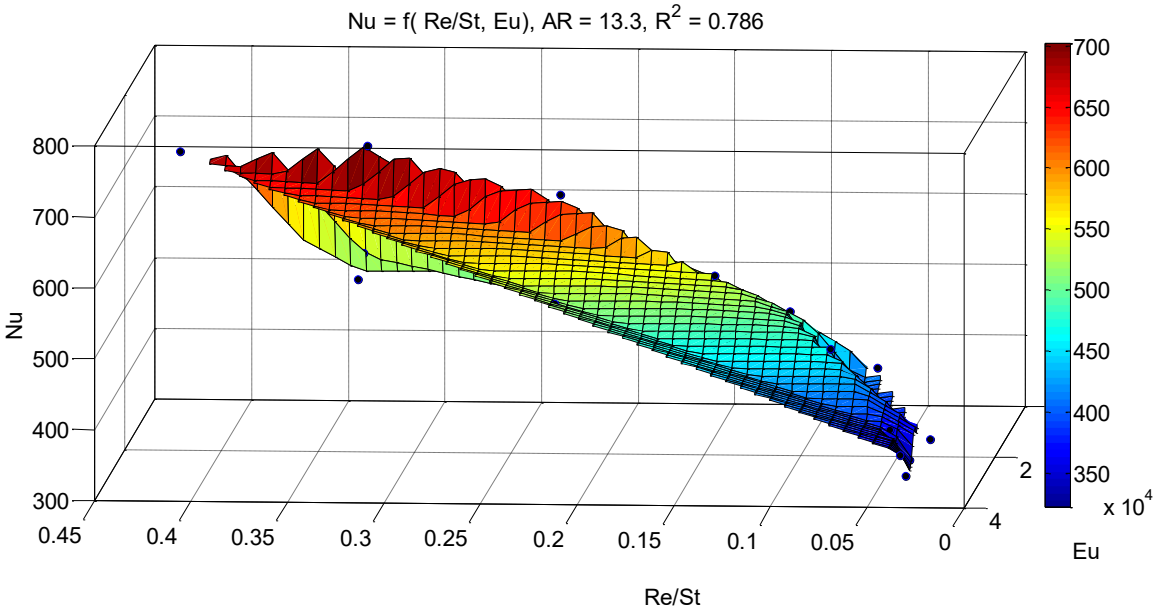

Figure 8.4 Three dimensional plot of the interpolating function for the relationship Nu = f (Re/St, Eu), AR = 6.4.

8.1.3 Correlations between the Re/St ratio and the Pr number

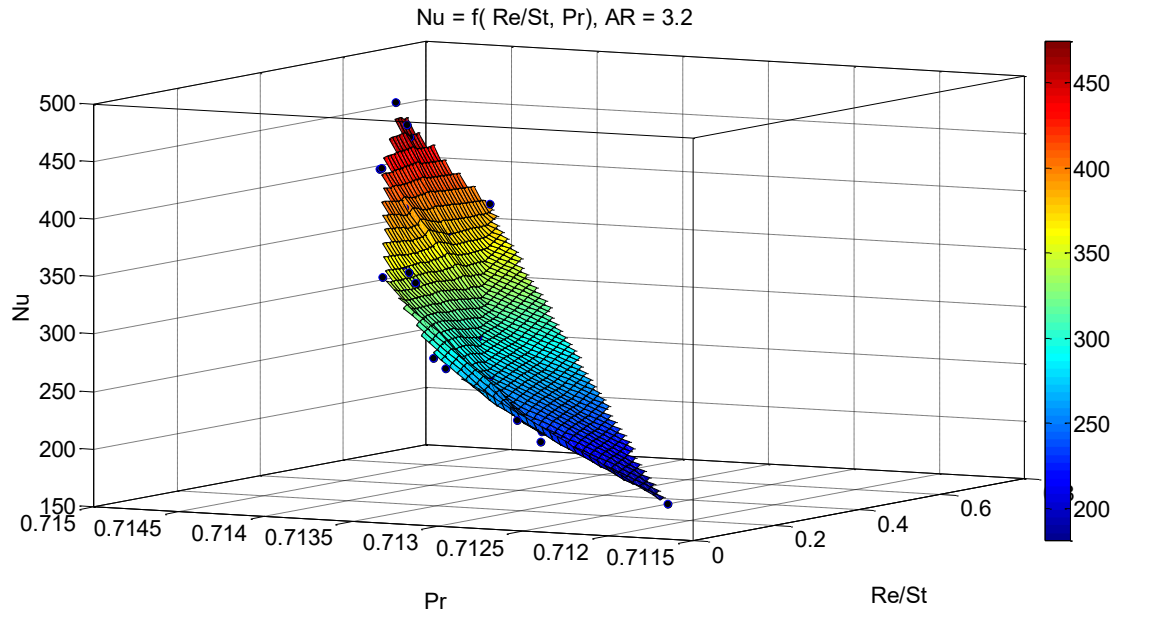

Figure 8.5 Three dimensional plot of the interpolating function for the relationship Nu = f (Re/St, Pr), AR = 3.2.

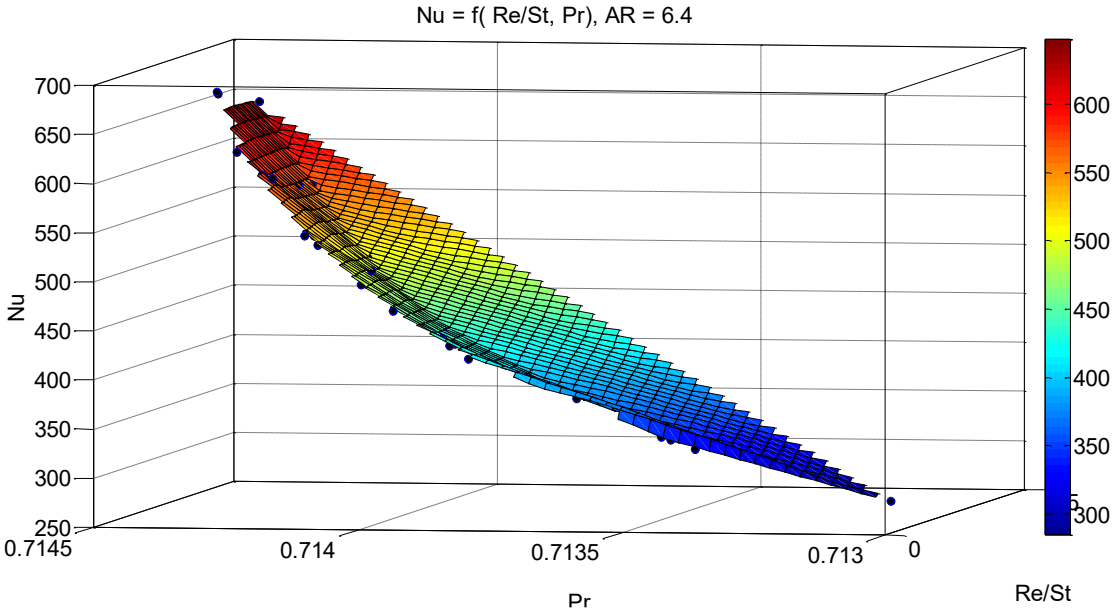

Figure 8.6 Three dimensional plot of the interpolating function for the relationship Nu = f (Re/St, Pr), AR = 6.4.

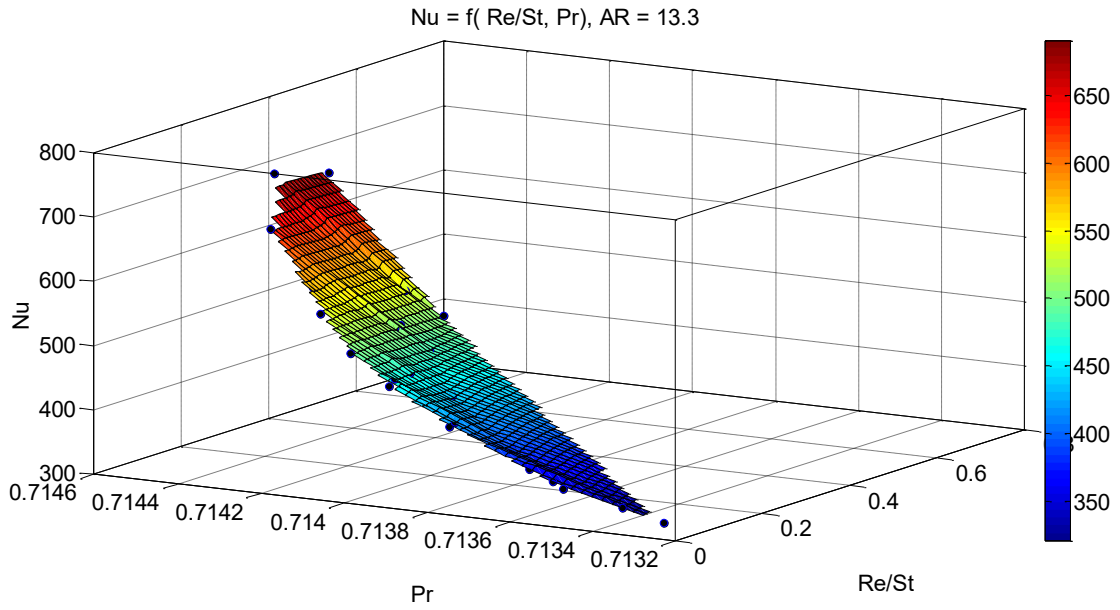

Figure 8.5 Three dimensional plot of the interpolating function for the relationship Nu = f (Re/St, Pr), AR = 13.3.

$$Nu_{AR1} = R_{10} + R_{11}\frac{Re}{St} + R_{12}Pr + R_{13}\left(\frac{Re}{St}\right)^2 + R_{14}\left(\frac{Re}{St}\right)Pr + R_{15}Pr^2 \quad (7.8)$$

$$Nu_{AR2} = R_{20} + R_{21}\frac{Re}{St} + R_{22}Pr + R_{23}\left(\frac{Re}{St}\right)^2 + R_{24}\left(\frac{Re}{St}\right)Pr + R_{25}Pr^2 \quad (7.9)$$

$$Nu_{AR3} = R_{30} + R_{31}\frac{Re}{St} + R_{32}Pr + R_{33}\left(\frac{Re}{St}\right)^2 + R_{34}\left(\frac{Re}{St}\right)Pr + R_{35}Pr^2 \quad (7.10)$$

Table 8.1 Summary of the polynomial coefficient relative to the interpolation of Nu = f(Re/St, Pr).

Correlation coefficients	Re/St	Pr
$R_{10} = 1.38x10^7$ $R_{11} = -1.966x10^5$	$R_{20} = 4.006x10^7$ $R_{21} = -3.899x10^5$	$R_{30} = 5.318x10^7$ $R_{31} = -3.077x10^5$

$R_{12} = -3.882x10^{7}$	$R_{22} = -1.125x10^{8}$	$R_{32} = -1.492x10^{8}$
$R_{13} = -338.4$	$R_{23} = -455.7$	$R_{33} = -347.3$
$R_{14} = 2.758x10^{5}$	$R_{24} = 5.463x10^{5}$	$R_{34} = 4.31x10^{5}$
$R_{15} = 1.38x10^{7}$	$R_{25} = 7.894x10^{7}$	$R_{35} = 1.047x10^{8}$

The above listed three dimensional curves were interpolated through a polynomial fit of degree two per each of the independent variables $\frac{\Re}{St}$ and Pr, with a coefficient of determination equal to 0.999, showing consistency and confirming the similarities, under the assumptions expressed for the synthetic jet in the non-dimensional modeling part.

It is also worth to notice that the $\frac{\Re}{St}$ ratio effectively represents the dominant non-dimensional parameter in characterizing the synthetic jet behavior, hypothesis confirmed for a generic synthetic jet by Utturkar et al. [2]. This is particularly due to the fact that the diameter of the jet simplifies between the numerator and the denominator of its expression, therefore not entering in the expression of its calculation.

With the experimental setup of this thesis work the peak of the synthetic jet performances has been identified to be at:

$$\frac{Re}{St} = 0.35 \tag{7.11}$$

Furthermore, the accurate evaluation of the changes in the thermodynamic properties of air as described in section , confirms what intuition suggested and the accuracy of the measurements. Even in the approximation of dry air, it is possible evidence the monotonic pattern of the Nu number observed along the Pr axis, which means clearly that, being sound wave essentially adiabatic as stated in section, the cooling effect is essentially due to the boundary layer redevelopment on the target plate. As Nu increases, so does Pr, which is indicative of a slight increase of momentum diffusivity with respect to thermal diffusivity, recalling that a pulsating flow causes accumulation effects that determine a slight increase in kinematic viscosity, simultaneously affecting the fluid conductivity. At the same time it must be recalled that a drop in the thermal diffusivity can very easily be overcome by a slight increase in the operating frequency, as it was highlighted in equation (2.16).

8.1.4 Effects of the Eu and Re acoustic numbers on the Nusselt number

The previous estimations of the synthetic jet performances were obtained through an energy-based approach that allowed for the determination of the pressure and

the velocity over the target plate, being the frequency known from the waveform generator, modeling the sound source as a point source with the above mentioned characteristics. This allows for the extension of the results to any device working under appropriate conditions of geometric and fluid dynamics similarity.

For the case of characterizing this particular synthetic jet, it has been appropriate to use the Reynolds acoustic definition [11], where the diameter plays a major role in determining the regime of the system. It has been proven to characterize well the system and identify peaks of heat transfer enhancement in relation to the acoustic power radiated by the loudspeaker (Eq. 7.12).

$$Re_{ac} = \frac{\rho \omega d^2}{\mu} \tag{7.12}$$

Nevertheless, this whole work has been founded by A*STAR with the purpose to implement solutions for the market of electronics cooling. Particularly, SIMTech has a lot of partnerships with manufacturing industries. Thus, between the scopes of the work there is the elaboration of a map that allows for the characterization of the heat transfer enhancement over the plate with a specific speaker, too. In this case, only the hypothesis of geometric similarity of the system has been conserved, while it was found interesting to determine the pattern of the Nusselt number with a correction that allowed for the evaluation of the sound source as it has been modeled in the previous paragraphs, considering the speakers dynamics, too.

Particularly, the value added of this analysis is that the evaluation of the power of the speaker has not been determined by modeling the speaker as an acoustic point source with a certain frequency, SPL etc. Rather as a function of the hardware available.

The output hereby reported proves that it is possible to easily identify heat transfer enhancement for a specific speaker (and experimental setup to a certain extent) in conditions of acoustic and geometric similarity with this thesis work**,** Beranek [9] p.124, 230.

$$W_{sp} = \frac{2V_{sp}B^2 l^2 \mathrm{R}_{MR}}{\left(R_g + R_e\right)^2 \left({R_M}^2 + {X_M}^2\right)} \tag{7.13a}$$

$$\mathrm{R}_{MR} = \frac{0.1886 a^6 \rho_0 \omega^4}{c^3} \tag{7.13b}$$

$$R_M = \frac{B^2 l^2}{R_g + R_e} + 2\mathrm{R}_{MR} + R_{MS} \tag{7.13c}$$

$$M_{M1} = 2.67 a^3 \rho_0 \tag{7.13d}$$

$$C_{MS} = \frac{1}{\omega_0{}^2(M_{MD} + M_{M1})} \tag{7.13e}$$

$$X_M = \omega(M_{MD} + 2M_{M1}) - \frac{1}{C_{MS}} \tag{7.13f}$$

with:

V_{sp} = voltage of the generator, [V];
R_g = generator resistance, [Ω];

R_e= resistance of voice coil in electrical ohms, measured with the voice coil movement blocked, [Ω];
ω = loudspeaker circular operating frequency, [rad/s];
ω_0 = loudspeaker circular resonance frequency, [rad/s];

B = steady air-gap flux density, [W/m^2];
l = length of wire on the voice-coil winding, [m];

M_{M1} =mass contributed by the air load on the sides of the piston for the frequency range, [kg];

M_{MD} = mass of the diaphragm, [kg];

a = loudspeaker diameter, [m];
R_{MR} = mechanical air-load resistance for both sides of an unbaffled loudspeaker, [Ω];

X_M = mechanical reactance (low frequency estimation), [Ns/m];
C_{MS} = total mechanical compliance of the loudspeaker suspensions, [m/N];

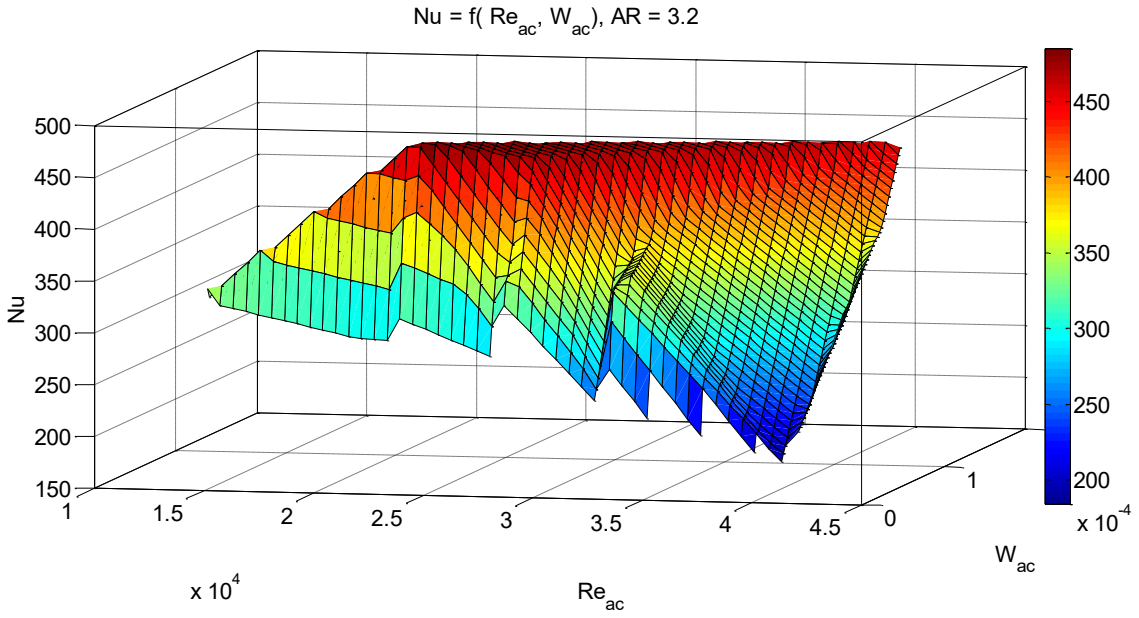

Figure 8.6 Three dimensional plot of the interpolating function for the relationship Nu = f (REac, Wac), AR = 3.2.

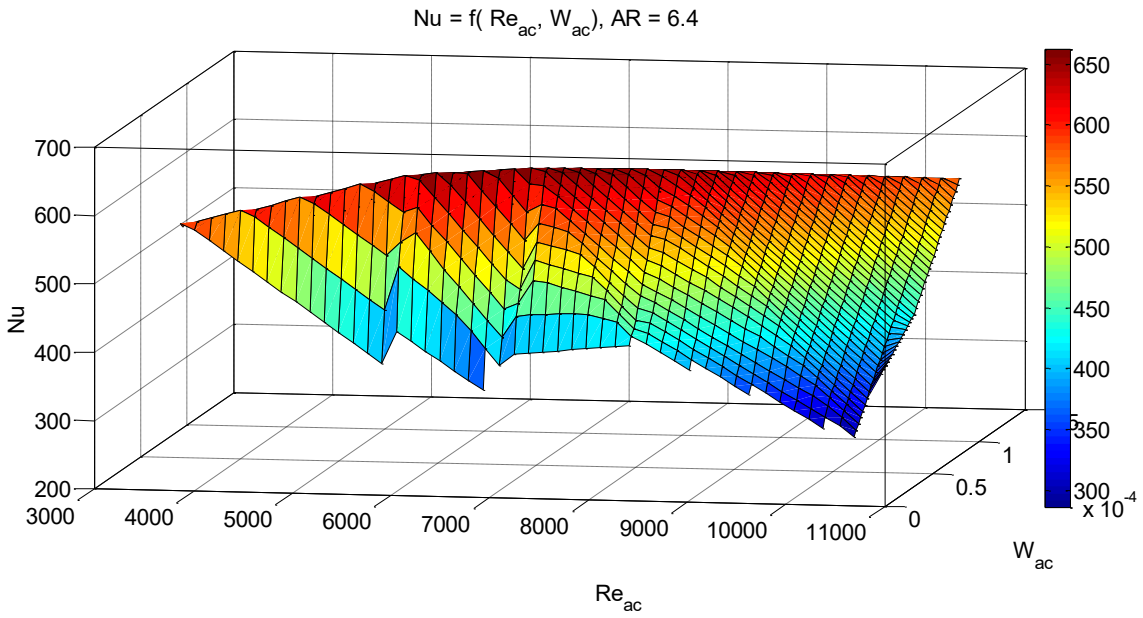

Figure 8.7 Three dimensional plot of the interpolating function for the relationship Nu = f (REac, Wac), AR = 6.4.

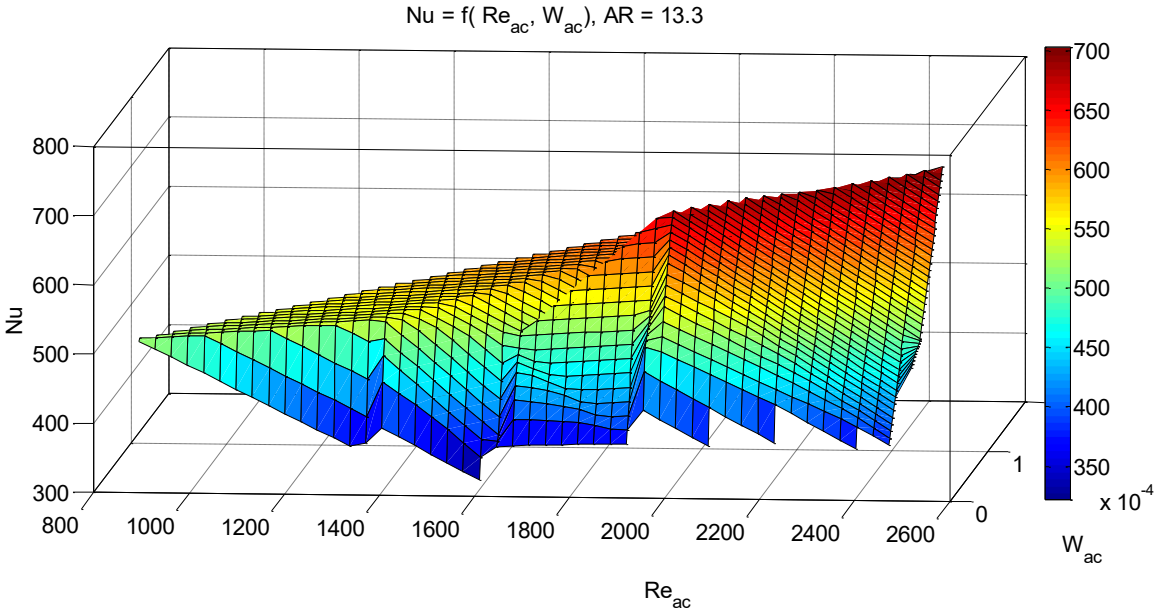

Figure 8.8 Three dimensional plot of the interpolating function for the relationship Nu = f (REac, Wac), AR = 13.3.

The abrupt change in the convection regime observed only for the AR = 13.3, located at the transition region (1700 $\leq Re_{ac} \geq$ 2000) is significant because recalls the importance of the stagnation point. Ideally, the stagnation point placed at the centre of the plate, plays a big role in determining the temperature over the plate, up to the point of overcoming the effect of the reduction in the plate area exposed to the synthetic jet. The air stagnating in axis with the synthetic jet centerline determines a differentiation of the temperature within the boundary layer, being its redevelopment obstacles in correspondence of the center of mass of the plate, as its thickness can be neglected. Subsequently the overall thermal exchange is

enhanced, as non-uniform heat transfer determines higher Nusselt numbers with respect to the uniform ones.

Nevertheless, it only happens after a certain $\mathfrak{R}_{ac}$ because the information of the pressure perturbation is obstacled by the presence of a small nozzle, increasing the tendence to determine accumulation effects, especially considering that the synthetic jet is close to the loudspeaker membrane, where the acoustic impedance becomes largely reactive.

9| CONCLUSION

9.1.1 Potential future improvements

As this experimental work has been started on purpose together with this specific thesis work, the author had a great chance to "learn by doing" and to sharpen intuition and problem solving skills. More importantly, it was needed to implement quick solutions within different fields of engineering: design, manufacturing, machining, implementation of experimental protocols, modeling and data processing. Thus, the author strongly encourages those who are interested in investing in their personal development in those competencies and aiming for multitasking positions in their future.

Some of the design issues that came up to light during the experimental part of the work at SIMTech were fixed, while on the other end various still need improvements.
With particular regard to the experimental set up, the implementation of the following solutions is strongly encouraged for the prosecution of this work, in ascending priority order:

1) the usage of a microphone for a more accurate evaluation of the pressure perturbation over the target plate;
2) the substitution of the loudspeaker with a piezoelectric membrane would increase significantly the amount of data to be processed, guaranteeing a sensible extension of the operating point ranges, resulting in a more comprehensive non-dimensional analysis;
3) the substitution of the plate adjustment unit to allow for a wider variety of aspect ratio to test;
4) the substitution of PLA with a more thermally stable material for the plate holder;
5) a better match between the output impedance of the waveform generator and the connected load impedance, as the greater the mismatch the higher the possibility to affect the performance of the driver . Particularly, the latter could determine higher currents in the loudspeaker voice coil than those that should carry. Consequently, SPL and impedance curves are not well replicated in reality and it becomes difficult to model the loudspeaker itself, as it leads to drop in velocities, increase in the SPL and shift of the resonance frequency;

6) insertion of the system in an anechoic chamber would refine the measurements, especially those that are related to pressure fluctuations within the sound field.

Bibliography

[1] A. Glezer,M.Amitay, «Synthetic jets,» Annual Review of Fluid Mechanics, vol. 34, pp. 503-529, 2002.

[2] K. Hamad,M. Kaseem, H.W. Yang, F. Deri, Y. G. Ko, «Properties and medical applications of polylactic acid: A review,» eXPRESS Polymer Letters, vol. 9, n. 5, pp. 435-455, 2015.

[3] R.W. Fox,P.J. Pritchard, A.T. McDonald, «Introduction to Fluid Mechanics,» John Wiley & Sons, Inc., 2009, p. 305.

[4] Y. Utturkar, R. Holman, R. Mittal,B. Carroll, M. Sheplak, L. Cattafesta, «A jet formation criterion for synthetic jet actuators,» AIAA Paper, n. 2003-0636, 2003.

[5] B.L. Smith, A.Glezer, «The formation and evolution of synthetic jets,» Phys. Fluids, vol. 10, n. 9, pp. 2281-2297, 1998.

[6] A. Glezer, «The Formation of Vortex Rings,» Phys. Fluids, vol. 31, n. 12, pp. 3532-3542, 1998.

[7] B. L. Smith, G.W. Swift «Synthetic Jets at Large Reynolds Number and Comparison to Continuous Jets,» AIAA Paper, pp. 2001-3030, 2001.

[8] Thermophysical and transport properties of humid air at temperature range between 0 and 100 _C, P.T. Tsilingiris, Science Direct, Energy Conversion and Management 49 (2008) 1098–1110,

[9]Acoustics, Acoustical Society of America Beranek, 1954

[10] Acoustic measurements, John Wiley & Sons, Inc.,1949

[11] Acoustic aspects of synthetic jetgenerated by acoustic actuator, M. M Kanase et al., Journal of Low Frequency Noise,Vibration and Active Contro 1–17, 2018, DOI: 10.1177/1461348418757879, journals.sagepub.com/home/lfn

LIST OF FIGURES

LIST OF TABLES

LIST OF EQUATIONS

Eq. 7.1 Mechanical approach definition of the Re number

Eq. 7.2 Theoretical expression for the average space velocity at the synthetic jet, rms over half period

Eq. 7.3 Mechanical approach definition of average space velocity at the synthetic jet

Eq. 7.4 Sound intensity expression at for 1W/1m.

Eq. 7.5 Sound intensity expression according to power law decay.

Eq. 7.6 Determination of the local pressure through the energy-based approach.

Eq. 7.7 Polynomial expression for the interpolation of Eu = f(Re/St, Pr).

Eq. 7.8 Polynomial expression for the interpolation of Nu = f(Re/St, Pr) for AR = 3.2.

Eq. 7.9 Polynomial expression relative to the interpolation of Nu = f(Re/St, Pr) for AR = 6.4.

Eq. 7.10 Polynomial expression relative to the interpolation of Nu = f(Re/St, Pr) for AR = 13.3.

Eq. 7.11 Synthetic jet characterization Re/St.

Eq. 7.12 Reynolds acoustic number definition.

Eq. 7.13a-f Theoretical formulas for the loudspeaker acoustic power [9].